

Structure-Based Design of AG-946, a Pyruvate Kinase Activator

Tao Liu,^[a] Anil K. Padyana,^[b] Evan T. Judd,^[c] Lei Jin,^[d] Dalia Hammoudeh,^[e] Charles Kung,^[f] and Lenny Dang^{*[g]}

Pyruvate kinase (PK) is the enzyme that catalyzes the conversion of phosphoenolpyruvate and adenosine diphosphate to pyruvate and adenosine triphosphate in glycolysis and plays a crucial role in regulating cell metabolism. We describe the structure-based design of AG-946, an activator of PK isoforms, including red blood cell-specific forms of PK (PKR). This was designed to have a pseudo-C₂-symmetry matching its allosteric binding site on the PK enzyme, which increased its potency toward PKR while reducing activity against off-targets observed from the original scaffold. AG-946 (1) demonstrated activation of human wild-type PK (half-maximal activation concentration

[AC₅₀] = 0.005 μM) and a panel of mutated PK proteins (K410E [AC₅₀ = 0.0043 μM] and R510Q [AC₅₀ = 0.0069 μM]), (2) displayed a significantly longer half-time of activation (> 150-fold) compared with 6-(3-methoxybenzyl)-4-methyl-2-(methylsulfinyl)-4,6-dihydro-5H-thieno[2',3':4,5]pyrrolo[2,3-d]pyridazin-5-one, and (3) stabilized PKR R510Q, an unstable mutant PKR enzyme, and preserved its catalytic activity under increasingly denaturing conditions. As a potent, oral, small-molecule allosteric activator of wild-type and mutant PKR, AG-946 was advanced to human clinical trials.

Introduction

Mature red blood cells (RBCs) rely primarily on glycolysis for energy production.^[1] As shown in Figure 1, the RBC-specific form of pyruvate kinase (PKR) catalyzes the final step of glycolysis in RBCs, converting phosphoenolpyruvate (PEP) to pyruvate, with concomitant formation of the energy carrier molecule adenosine triphosphate (ATP).



Figure 1. Role of PK in glycolysis.^[1] ADP = adenosine diphosphate; ATP = adenosine triphosphate; DPG = diphosphoglycerate; FBP = fructose 1,6-bisphosphate; PEP = phosphoenolpyruvate; PG = phosphoglycerate; PK = pyruvate kinase. Note: Not all steps of glycolysis are shown.

Decreased pyruvate kinase (PK) function leads to dysfunctional RBCs with defective glycolysis, including increased levels of 2,3-diphosphoglycerate (2,3-DPG) and PEP and decreased levels of ATP.^[2] Thus, because PK increases the amount of ATP produced, this is a key enzyme for maintaining energy homeostasis in erythrocyte precursors and RBCs.

The activity of wild-type (WT) PK can play a role in hemolytic anemias where PK function may become critical because of increased energy demands, increased cellular oxidative stress, or the abnormal accumulation of upstream glycolytic metabolites (i. e., 2,3-DPG). For instance, a study on RBCs from patients with sickle cell disease (SCD) demonstrated reduced PK activity and stability compared with RBCs from healthy subjects.^[3]

Myelodysplastic syndromes (MDS) are a heterogeneous group of bone marrow disorders characterized by dysfunctional hematopoiesis, progressive cytopenia, and abnormal cellular maturation.^[4] Samples from patients with MDS, but not from patients with other myeloid malignancies, have shown acquired deficiency of PK activity.^[5] More recently, studies using RBCs from patients with lower-risk MDS found decreased glycolytic activity in these patients, including reduced PK activity and ATP levels compared with healthy counterparts.^[6] Moreover, PK activation by mitapivat has demonstrated clinical improvement in anemia in patients with thalassemia, a disease of ineffective erythropoiesis with features that share similarities with MDS-

[a] Dr. T. Liu
Ensem Therapeutics
880 Winter St, Waltham, MA 02451, USA

[b] Dr. A. K. Padyana
Atavistik Bio.
75 Sidney St, Cambridge, MA 02139, USA

[c] Dr. E. T. Judd
Novartis Institute for Biomedical Research
250 Massachusetts Ave, Cambridge, MA 02139, USA

[d] Dr. L. Jin
Agiros Pharmaceuticals, Inc.
88 Sidney St, Cambridge, MA, USA

[e] Dr. D. Hammoudeh
Agiros Pharmaceuticals Inc.,
88 Sidney St, Cambridge, MA, USA

[f] Dr. C. Kung
Remix Therapeutics
100 Forge Rd, Watertown, MA 02472, USA

[g] L. Dang
Verolix, Inc.
800 Boylston St. Unit 900147, Boston, MA, 02199, USA
E-mail: lenny.dang@gmail.com

Supporting information for this article is available online at <https://doi.org/10.1002/cmdc.202300559>

© 2023 Agios Pharmaceuticals. ChemMedChem published by Chemistry Europe and Wiley-VCH GmbH. This is an open access article under the terms of the Creative Commons Attribution License, which permits use, distribution and reproduction in any medium, provided the original work is properly cited.

associated anemia.^[7] Therefore, enhancement of glycolysis through PK activation may improve the survival and differentiation of erythroid precursors in the bone marrow and may also improve RBC functionality in peripheral circulation, and thus has the potential to treat MDS-associated anemia.

In addition to its central role in producing ATP, PK is also a key regulator of 2,3-DPG levels in RBCs; when bound to hemoglobin, 2,3-DPG decreases its affinity for oxygen, manifested as a right-shift in the hemoglobin–oxygen dissociation curve.^[8] While this normal physiologic effect of 2,3-DPG facilitates oxygen delivery to tissues, it can be deleterious in patients with SCD as the deoxygenated form of sickle hemoglobin (HbS) has a much higher propensity to sickle.^[8–9] Therefore, by regulating 2,3-DPG and ATP levels, PK activation can potentially reduce RBC sickling in patients with SCD. PK activation has been shown to decrease RBC 2,3-DPG levels and increase ATP levels in both preclinical models and humans.^[6b,10] The inheritance of a single mutant allele of the *PKLR* gene (i.e., the gene that codes for PK) can result in more severe forms of hemolytic anemia. Carriers of a single allele of HbS are usually asymptomatic, but a patient bearing a single HbS allele as well as a mutant *PKLR* allele can suffer from a severe phenotype of SCD.^[11]

Herein, we report the structure-based design and optimization of the clinical candidate compound **27** (AG-946), from a chemical starting point that was originally identified by the National Institutes of Health chemical genomics center.^[12]

Results and Discussion

Binding Mode of the Tricyclic Core in Human PKR Enzyme

Two of the reported thieno[2',3':4,5]pyrrolo[2,3-d]pyridazin-5-one compounds, **1** and **2** (Figure 2A), were synthesized and tested in multiple different *in vitro* biochemical and biophysical activity assays and in co-crystallization experiments.^[12] Compounds **1** and **2** showed potency in activating the recombi-

nantly expressed human WT PKR enzyme (half-maximal activation concentration $[AC_{50}] = 0.038 \mu\text{M}$ and $0.032 \mu\text{M}$, respectively). The co-crystal structure of compound **2** with the WT human PKR protein at 2.35 Å resolution (Figure 2B) shows compound **2** binding in an allosteric pocket at the dimer interface, distinct from the fructose 1,6-bisphosphate (FBP) binding site. Compound **2** binding is mediated by π – π sandwich interactions of the thienopyrrolopyridazinone tricyclic core with two F69 residues from two adjacent monomers. The 3-methoxyphenyl ring is in an almost perpendicular conformation to the tricyclic ring system, forming a π -edge interaction to residue F69 and forming van der Waals interaction with L437. Based on the observed interactions, we hypothesized that the highly constrained tricyclic ring system is critical for the activity of compound **2**. We first explored the structure activity relationship (SAR) in this core region with the aim of developing a potent PK activator.

Pyridazinone Ring Modification

Substituting the pyridazinone of compound **1** with other six-membered aromatic ring systems, such as phenyl (compound **3**) or pyrimidinone (compound **4**) rings (Figure 3A), resulted in a loss of PKR activation (Table 1), indicating that not any tricyclic core structure can form π – π interactions with the two F69 residues.

Replacing the pyridazinone with the five-membered dihydro-pyrrol-2-one (compound **5**) restored potency compared with compounds **3** and **4** but was 100-fold less potent than compound **1**. From the crystal structure of Figure 2B, residue Q436 of one monomer is adjacent to position N12 of the pyridazinone ring. The distance between N12 and the protein surface is $\sim 3.4 \text{ \AA}$, insufficient for the CH group of compounds **3** and **4**. Interestingly, the CH group was tolerated at position 13 of the pyridazinone owing to a small pocket between the two Q436 residues. The smaller dihydro-pyrrol-2-one is unlikely to result in steric clashes with the binding site; however, the partially saturated five-membered ring is less ideal for forming

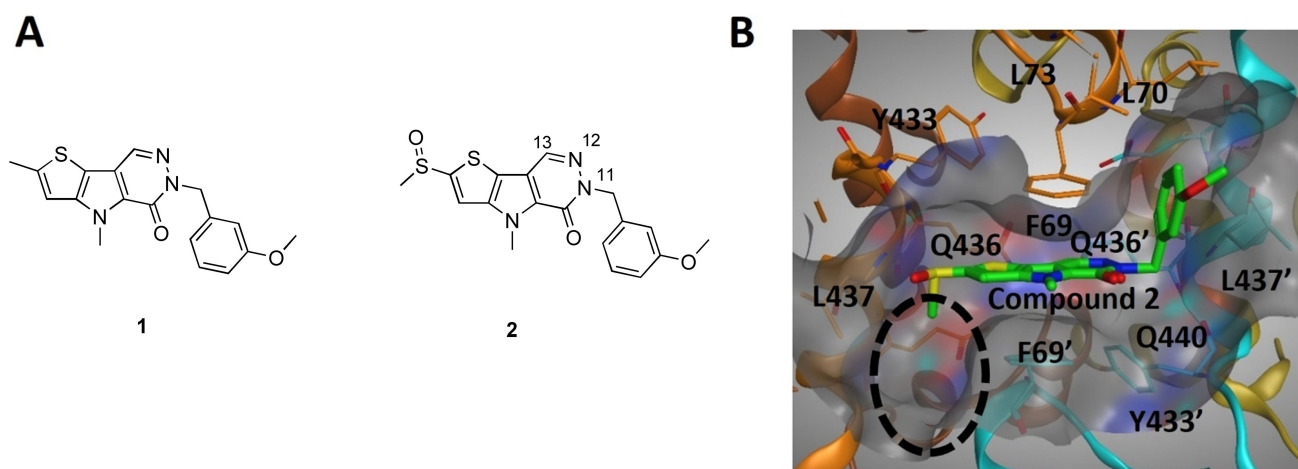


Figure 2. Literature compounds **1** and **2** (A) and co-crystal structure of compound **2** (green) with human PKR, showing the allosteric binding site at the dimeric interface (B). Two conformations of compound **2** flipped head-to-toe were modeled in the binding site. For clarity, only one of the conformations is presented. PKR = red blood cell-specific form of pyruvate kinase.

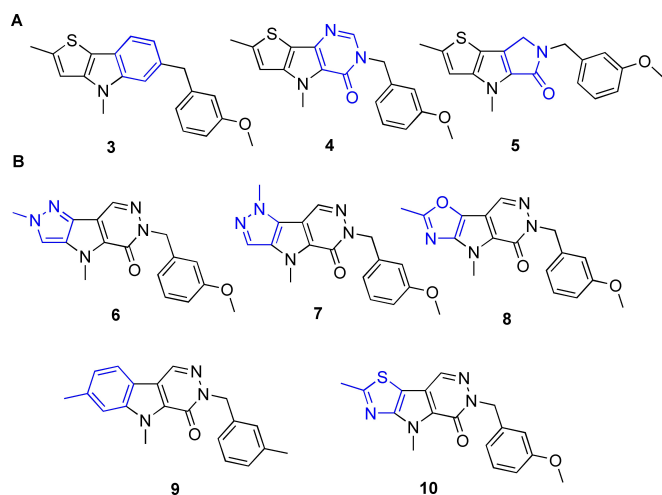


Figure 3. Compounds 3–5 explore various substitutions of the center ring system (A) and analogs 6–10 examine alternatives to the thiophene ring of compound 1 (B).

Compound ID	PKR AC ₅₀ (μM)
1	0.038
3	> 100
4	38
5	3.78

AC₅₀ = half-maximal activation concentration; ID = identification; PKR = red blood cell-specific form of pyruvate kinase.

the π - π interactions with the F69 residues from two different monomers. Based on initial SAR, we maintained the pyridazinone ring in subsequent analogs.

Design and Synthesis of Thiazolopyrrolopyridazinone Core

Compound 1 contains a thiophene ring, which is known for its cytochrome P450-catalyzed reactive metabolism derived from thiophene ring oxidation.^[13] Thus, we focused on replacing the thiophene ring to increase metabolic stability and synthesized compounds 6–10 (Figure 3B).

Of the new analogs, pyrazole (compounds 6 and 7), oxazole (compound 8), and the phenyl analog (compound 9) had negative impacts on the SAR, while the thiazole analog (compound 10) was almost equipotent to compound 1 (Table 2). The trisubstituted thiazole ring is more electron-deficient than the thiophene ring because incorporation of electronegative nitrogen atoms in an aromatic heterocycle typically decreases its overall electron density, as well as the energy of the highest occupied molecular orbital, making the heterocycle less prone to P450-mediated oxidative metabolism.^[14] Therefore, the thiazolopyrrolo-pyridazinone was chosen as the pharmacophore for further optimization.

Table 2. Human PKR activity of compounds 1 and 6–10.

Compound ID	PKR AC ₅₀ (μM)	Cell-based ATP AC ₅₀ (μM)
1	0.038	ND
6	9.619	ND
7	No fit	ND
8	2.573	ND
9	0.473	ND
10	0.093	0.476

AC₅₀ = half-maximal activation concentration; ATP = adenosine triphosphate; ID = identification; ND = not determined; PKR = red blood cell-specific form of pyruvate kinase.

Developing Pseudo-C2-Symmetric Analogs for the Two-Fold Symmetric Binding Pocket

The pocket where compound 2 binds is two-fold symmetric due to its location at a homodimerization interface (Figure 2B). The crystal structure of PKR with compound 2 shows two alternative binding modes for compound 2, likely due to partial occupancy along the pseudo-two-fold symmetry with methoxyphenyl occupying the pockets in both ends (Supplementary Figure 1). In the binding pose modeled (Figure 2B), the top right corner of the pocket is occupied by the 3-methoxyphenyl group, while the bottom left-hand corner (Figure 2B, dashed circle) is left unoccupied. This led us to further optimize the tricyclic compound and synthesize a C2-symmetric molecule to maximize the interaction to the C2-symmetric binding pocket.

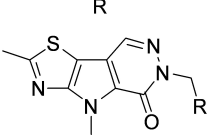
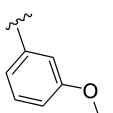
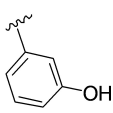
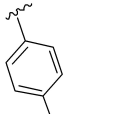
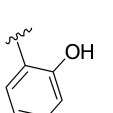
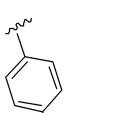
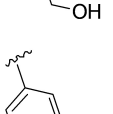
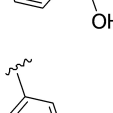
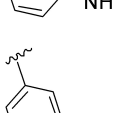
In vitro profiling of compound 2 showed phosphodiesterase (PDE) 3 inhibition at low μM ranges (half-maximal inhibitory concentration [IC₅₀] 1.25 μM and 1.32 μM against PDE 3A and PDE 3B, respectively). To understand this off-target activity, we analyzed the published crystal structure of PDE inhibitor MERCK1 (IC₅₀ 0.27 nM)^[15] in complex with PDE 3B (Supplementary Figure 2). This showed that MERCK1 binds in a long and flat pocket of PDE 3B. The left-hand side of the pocket is closed, while the right-hand side is opened to the solvent front. In the right-hand side pocket, there is a key π - π interaction between the phenyl ring of MERCK1 with the F991 residue of PDE 3B. It may be possible that compound 2 binds to this PDE 3B-binding pocket. On the other hand, a C2-symmetric molecule would no longer fit this PDE-binding pocket. Therefore, we rationalized that designing C2-symmetric molecules could optimize interactions with the PKR binding pocket and reduce the potential for off-target PDE 3 liability.

SAR to Explore the Right-hand Side of the Pseudo-C2-Symmetric Molecule

After the tricyclic core was settled as a thiazolopyrrolopyridazinone, we decided to optimize the functional groups on both sides of the core to make a pseudo-C2-symmetric molecule.

First, the right-hand side was refined to maximize the interaction between the right-hand-side ring with nearby amino acids, especially the D397 residue (Table 3 and Figure 4). To explore single point changes, the left-hand side was kept as the methylthiazole group. Compounds 11–17 were synthesized. Removing the methyl from the methyl ether of compound 10 increased the potency about five-fold (compound 11). Interestingly, compound 12, with the phenol group at the 4 position, was equipotent to compound 11; however, the 2-position isomer, compound 13, was significantly less potent. We

Table 3. Compounds for the right-hand-side SAR exploration.

R	PKR AC ₅₀ (μM)	Cell-based ATP AC ₅₀ (μM)	Cell-based PKR activity AC ₅₀ (μM)
			
10 	0.093	0.476	ND
11 	0.017	0.093	0.19
12 	0.018	ND	ND
13 	0.373	2.573	ND
14 	3.298	8.049	ND
15 	0.044	0.208	1.307
16 	0.012	0.061	0.23
17 	1.642	3.368	ND

AC₅₀ = half-maximal activation concentration; ATP = adenosine triphosphate; ID = identification; ND = not determined; PKR = red blood cell-specific form of pyruvate kinase; SAR = structure activity relationship.

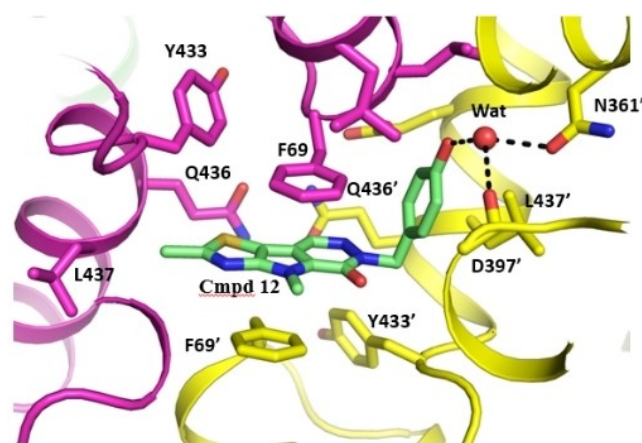


Figure 4. Co-crystal structure of compound 12 (green) bound to PKR. Cmpd = compound; PKR = red blood cell-specific form of pyruvate kinase; Wat = water.

determined the co-structure of compound 12 with the human PKR to understand the SAR and guide further optimization (Figure 4). The crystal structure showed a hydrogen bond donor/acceptor interaction hosted by the 4-phenol OH group and mediated through water with the main-chain carbonyl group of D397 and the side chain of N361. Interestingly, when we extended the hydroxy group to one more carbon at the 4 position (compound 14), potency was significantly reduced.

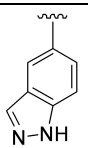
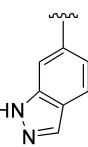
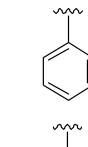
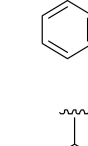
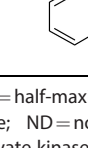
Compound 15 has a 1-carbon extension at the 3 position of the phenyl ring, causing a two-fold loss of activity compared with compound 11 (Table 3). This SAR showed that an aromatic ring with a hydrogen bond donor at the optimal position/orientation was preferred for potency. For reasons that are unclear to us, substituting the 3-phenol with 3-aniline (compound 16) resulted in potency similar to that of compound 11. The 4-aniline direct analog (compound 17) lost almost 100-fold potency compared with the 4-phenol compound 12.

Due to the potential liability of the phenol and aniline moieties,^[16] we sought an isosteric approach in an attempt to circumvent the potential liability. Indazole has been used as an isostere for phenol,^[17] so we synthesized compounds in this series to explore the SAR. As reported in the literature,^[18] 2-aminopyridine has been widely used in drug discovery programs as a substitute for aniline. Thus, compounds 18–22 were synthesized (Table 4). Among these compounds, analog 22 demonstrated the best potency of 0.022 μM, equipotent to the initial lead compound 16. This SAR exploration gave us the 2-aminopyridine as the optimal functional group on the right-hand side. Concurrent with optimization on the right-hand side of the molecule, we sought to further optimize the left-hand-side functional groups and fixed the right-hand side as 3-methoxyphenyl to explore single point changes.

SAR Exploration of the Left-hand Side of the Molecule

As shown in Table 5, compounds 23–26 were synthesized and tested for PKR binding, activation, and PDE 3B inhibition.

Table 4. Analogs 18–22 for the right-hand-side SAR exploration.

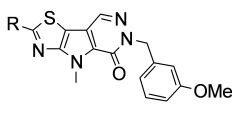
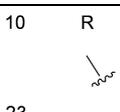
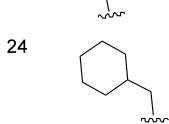
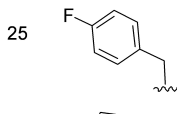
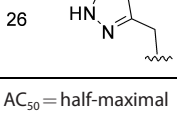
R	PKR AC ₅₀ (μ M)	Cell-based ATP AC ₅₀ (μ M)	Cell-based PKR activity AC ₅₀ (μ M)
	0.120	1.622	ND
	1.300	3.27	ND
	1.100	2.406	ND
	0.045	0.251	ND
	0.022	0.031	0.07

AC₅₀=half-maximal activation concentration; ATP=adenosine triphosphate; ND=not determined; PKR=red blood cell-specific form of pyruvate kinase; SAR=structure activity relationship.

Compared with the methyl group in compound **10**, the ethyl group in compound **23** reduced PKR binding potency. However, both compounds had better PDE inhibition profiles compared with compound **2**. A saturated aliphatic cyclic hydrocarbon, such as a cyclohexyl methyl group (compound **24**), was associated with a significantly reduced PKR binding potency but a significantly improved PDE 3B profile. The deterioration of the PKR binding potency could be due to the loss of the π -edge interaction with the F69 residue.

We then explored the addition of aromatic rings on the left-hand side of the molecule. Compound **25**, which is close to a pseudo-C₂-symmetric molecule, regained most of the PKR potency compared with compound **24**. At the same time, PDE 3B inhibition was completely mitigated. Leveraging the right-hand SAR, an aromatic ring with a hydrogen bond donor was thought to be an effective group for participating in the desired hydrogen bond donor/acceptor interaction. Compound **26**, with a pyrazolomethyl group on the left-hand side, was synthesized and demonstrated further improved potency of 0.014 μ M. Furthermore, compound **26** was devoid of PDE 3B inhibition (more than 100 μ M). Based on this SAR investigation, we concluded that the pyrazolomethyl group was optimized as the left-hand-side group.

Table 5. Analogs 10 and 23–26 for the left-hand-side SAR exploration.

R	PKR AC ₅₀ (μ M)	PDE 3B IC ₅₀ (μ M)	Cell-based ATP AC ₅₀ (μ M)	Cell-based PKR activity AC ₅₀ (μ M)
	0.093	14.692	0.476	ND
	0.200	29.645	1.191	ND
	3.200	> 100.000	> 10	ND
	0.139	> 100.000	0.645	ND
	0.014	> 100.000	0.15	0.021

AC₅₀=half-maximal activation concentration; ATP=adenosine triphosphate; IC₅₀=half-maximal inhibitory concentration; ND=not determined; PDE=phosphodiesterase; PKR=red blood cell-specific form of pyruvate kinase; SAR=structure activity relationship.

From the extensive SAR described, combining the 2-aminopyridine on the right-hand side with a pyrazolomethyl on the left-hand side led to compound **27** (Figure 5A), which was identified as the clinical candidate AG-946 for advancement in human clinical trials. Overall, compound **27** (AG-946) has a pseudo-C₂-symmetric shape, as shown in the crystal structure (Figure 5B). The thiazolopyrrolopyridazinone tricyclic core maintains π - π interaction with the two F69 residues from adjacent protomers. Combination of the best fragments in the right-hand side and the left-hand side enhances the molecular interactions for compound **27** (AG-946) by extending a number of additional contacts within the PKR dimer interface, explaining the enhanced potency. The aromatic rings of the 2-aminopyridinemethyl group and pyrazolomethyl groups host π -edge interactions with F69, van der Waals interaction with L437, and the key hydrogen bond interactions with D397. These groups also host additional water-mediated hydrogen bond interactions with N361 and D397. Compound **27** (AG-946) showed very good activity to WT PKR, K410E, and the prototypical unstable R510Q, as well as other mutant PKR enzymes (Figure 6).

Biochemical Characterization of Compound 27 (AG-946)

Compound **27** (AG-946) demonstrated good activity in cell-based assays using purified RBCs, with an average AC₅₀ for PKR activation of 35 \pm 12 nM and an average maximum percent PKR activation of 197 \pm 13% (N=13 experiments). The average AC₅₀ for increase in ATP levels was 17 \pm 7 nM, and the average

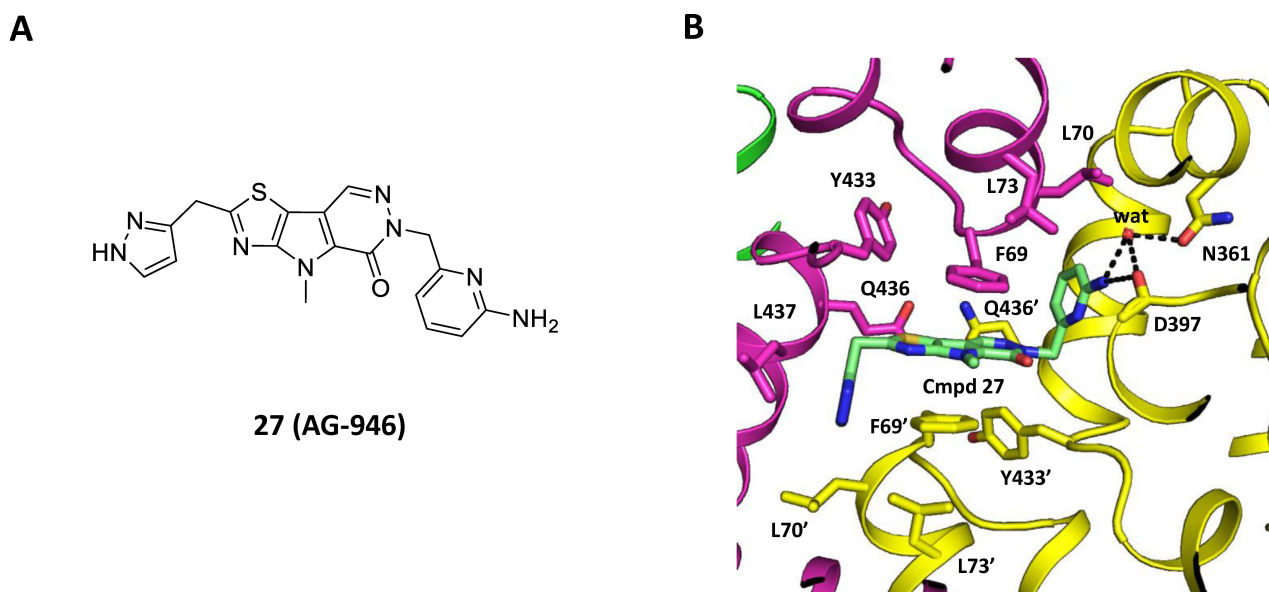


Figure 5. Compound 27 (A) and co-crystal structure of compound 27 (AG-946) bound to PKR with a bridged water interaction (B). Cmpd = compound; PKR = red blood cell-specific form of pyruvate kinase; Wat = water.

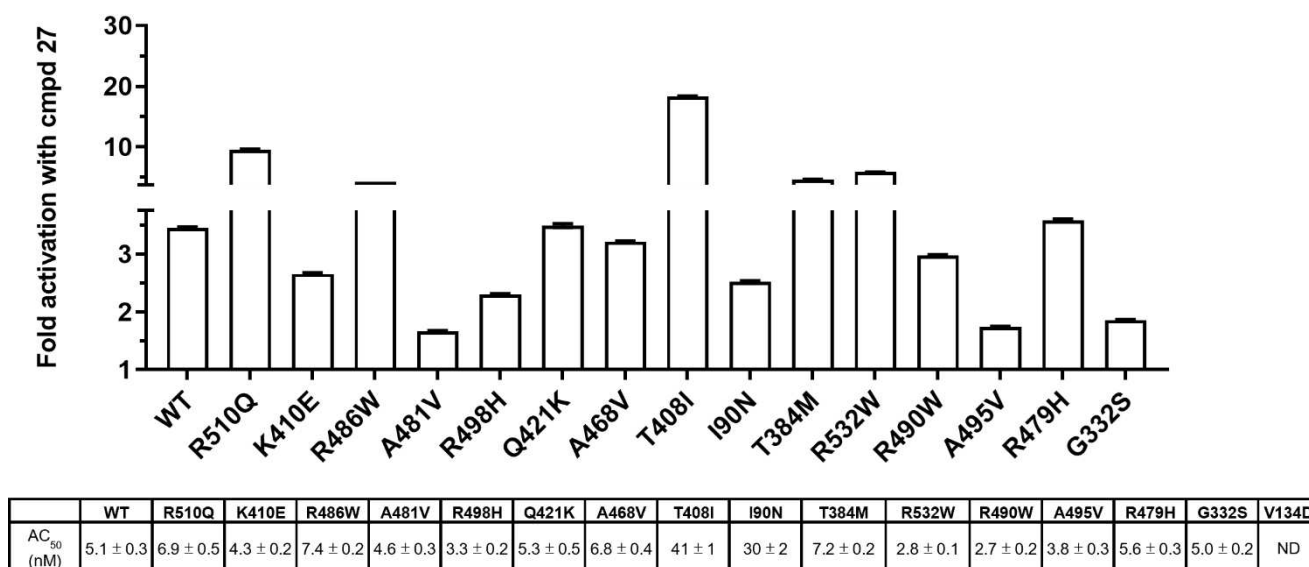


Figure 6. (Top) Bar graph depicting the fold activation of a panel of different PKR enzymes. Error bars represent the standard error of the mean. (Bottom) Relative potency and activation levels measured by dose response of compound 27 (AG-946) using an *in vitro* coupled enzymatic assay. AC₅₀ = half-maximal activation concentration; cmpd = compound; ND = not determined; PKR = red blood cell-specific form of pyruvate kinase; WT = wild-type.

percent increase in ATP levels was $145 \pm 8\%$ (N=21 experiments).

Compound 27 (AG-946) activated both WT PKR and a prototypically unstable PKR mutant, PKR R510Q (Figures 6 and Figure 7A). To investigate the lifetime of the induced activation of PKR by compound 27 (AG-946), activator-jump-dilution experiments were performed. In these experiments, PKR was preactivated with compounds and subsequently diluted to induce dissociation from the enzyme. The enzyme activity was measured over time to determine the rate constant associated with the loss of the activation (Figure 7B). Compound 27 (AG-946) elicited a dramatically improved half-life of activation (slow

observed rate of inactivation) compared with compound 2, suggesting that activation by compound 27 (AG-946) is longer-lived than activation by compound 2.

Our previous work demonstrated that PKR activators could also stabilize certain mutant forms of PK.^[19] A modified thermostability assay, which measures the ability of a compound to protect the catalytic activity of PKR when challenged with high temperatures and a chemical denaturant, was developed (Figure 7C). Compound titration in the chemo-thermostability assay yielded the potency of stabilization. Treatment with compound 27 (AG-946) resulted in a ~90-fold increase in the

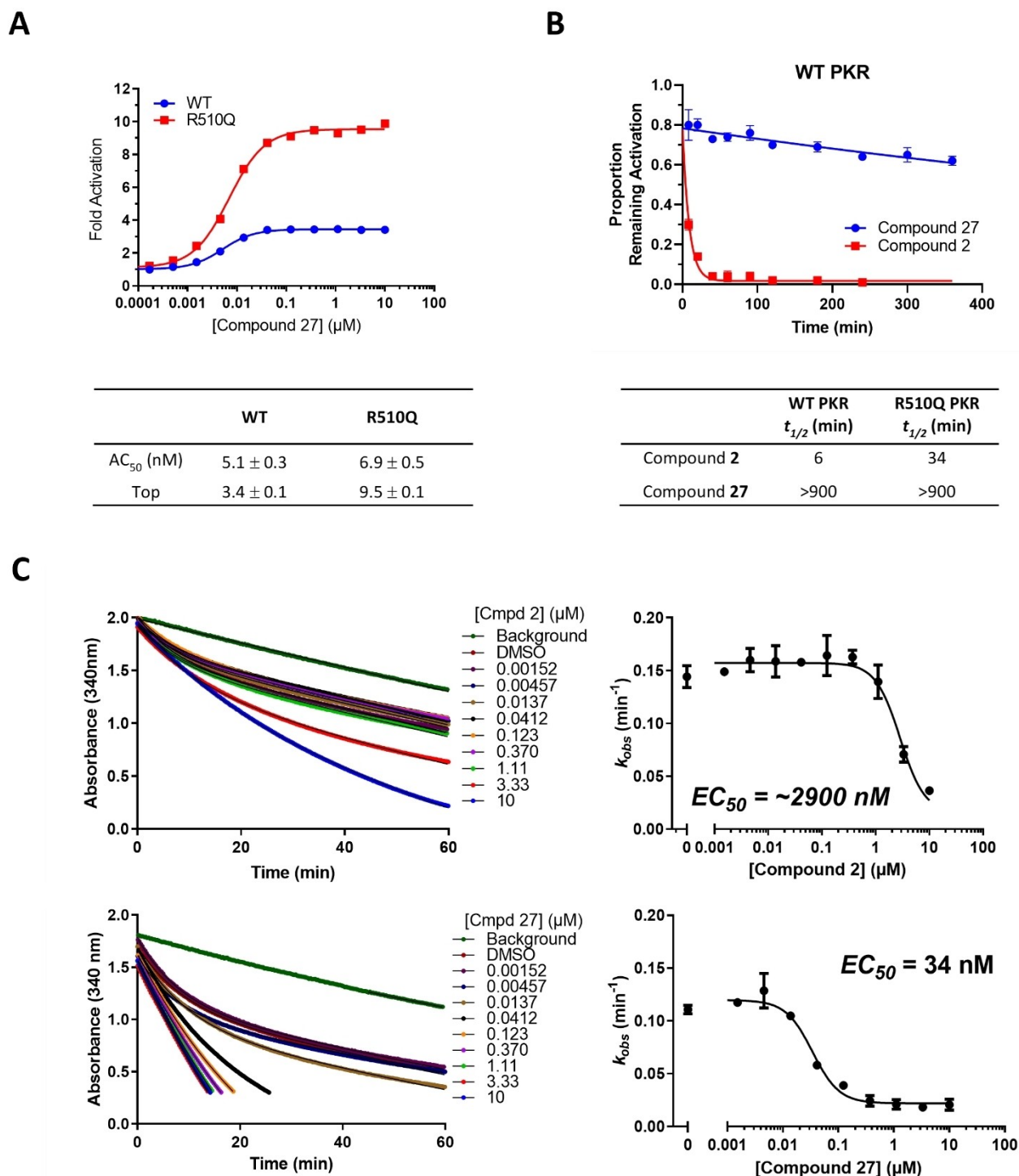


Figure 7. Relative potency and activation levels measured by dose response of compound 27 (AG-946) using an *in vitro*-coupled enzymatic assay (A) and half-life of PKR activation by compound 27 (AG-946) (B). WT (left) and R510Q (right) PKR enzyme forms were preactivated with the compound, then diluted into assay buffer, and activity measurements were taken at different time points. Data were normalized to account for loss of enzyme activity over time, then fit to a single exponential decay allowing for extraction of the half-life of activation. Measurement of the ability of compounds to stabilize PKR R510Q (C). Left panels show the progress curves recorded at different compound concentrations under destabilizing conditions. Right panels show k_{obs} as a function of compound concentration. AC₅₀ = half-maximal activation concentration; compd = compound; DMSO = dimethyl sulfoxide; EC₅₀ = half-maximal effective concentration; k_{obs} = rate of conversion; PKR = red blood cell-specific form of pyruvate kinase; t_{1/2} = half-life; WT = wild type.

potency of stabilization of PKR R510Q compared with compound 2 (Figure 7C).

The magnitude of stabilization of PKR R510Q by compound 27 (AG-946) was measured by modifying the chemo-thermostability assay such that a compound was held constant at the

concentration of 50 μM and the chemical challenge (guanidine hydrochloride [Gnd-HCl]) was gradually increased (Supplementary Figure 3). While the magnitude of stabilization by compound **2** gradually decreased (as indicated by increasing observed rates of inactivation) as the challenge was increased, compound **27** (AG-946) was more resistant to inactivation at higher Gnd-HCl concentrations, suggesting that the magnitude of activation, not just the potency, was larger for compound **27** (AG-946) than for compound **2**.

The *in vitro* metabolic stability of compound **27** (AG-946) was evaluated in mouse, rat, dog, monkey, and human microsomes. Compound **27** (AG-946) was stable in human microsomes, and intrinsic clearance in mouse, rat, dog, and monkey liver microsomes were 3.29, 2.21, 4.05, and 2.40 L/h/kg, respectively. In contrast, compound **12** was found to be highly unstable in human, mouse, and rat microsomes, with intrinsic clearance of 6.21, 55.70, and 20.40 L/h/kg, respectively.

In an off-target screening panel of 92 receptors, ion channels, enzymes, and transporters evaluated at 10 μM , no binding or enzymatic activity was inhibited by >50% for compound **27**.

Conclusions

Herein, we describe the discovery of compound **27** (AG-946), an investigational, potent, allosteric activator of PK with exceptionally long on-target residence time that has the potential to durably enhance RBC functionality and survival by increasing glycolysis and ATP production. The compound was optimized to have drug properties suitable for clinical development. The structure-based design effort leading to the identification of compound **27** (AG-946), based on a thieno-pyrrolo-pyridazinone chemical scaffold, focused on optimizing the spatial relationship between the C2 symmetry of the drug ligand and the binding pocket created by the obligatory two-fold symmetry of monosubunit dimerization in the tetrameric PKR enzyme. As a result, compound **27** (AG-946) achieves low nanomolar potency in both biochemical and cellular activity assays. A series of novel, biophysical, kinetic-based PK assays was developed to assess and guide medicinal chemistry design to identify compounds with the best ability to stabilize the mutant PKR R510Q (a prototypical unstable mutant), as well as to possess the long on-target residence time. Based on these criteria, compound **27** (AG-946) was selected for its high on-target activity and its capacity to stabilize both WT and unstable mutant PK proteins. Compound **27** (AG-946) was also optimized for improved selectivity, especially eliminating the undesirable off-target activity of PDE3 isoforms, which was identified early on as a liability, by taking advantage of well-described crystallographic structures of PDE isozymes. Overall, compound **27** (AG-946) represents a new investigational PK activator with potential for low projected human drug load and long pharmacodynamic duration of action, suitable for clinical development in a broad range of hemolytic anemias and diseases characterized by dyserythropoiesis. Compound **27** (AG-946) is currently being

evaluated in clinical trials for low-risk MDS (NCT05490446) and SCD (NCT04536792).

Experimental Section

Cloning, Protein Expression, and Purification. For crystallization, WT PKR₅₀₋₅₇₄ was cloned into a pET28a vector with an N-terminal 6xHis-tag and a thrombin cleavage site and expressed in *E. coli* strain BL21 (DE3) (Transgen), as described previously.²⁰ Harvested cells were lysed in phosphate-buffered saline (PBS), pH 7.4, containing protease inhibitors (Roche), and the protein was purified using Ni-nitrilotriacetic acid (NTA) (GE Healthcare) affinity chromatography. The 6xHis-tag was enzymatically cleaved with thrombin (Biosharp, 1,000 U) overnight and removed using Ni-NTA subtraction. Additional purification was performed by anion exchange (Resource Q, GE Healthcare) chromatography using a gradient of 0–1 M NaCl in PBS, pH 8.0. Tetrameric PKR₅₀₋₅₇₄ was concentrated to 23.0 mg/mL and flash-frozen in liquid nitrogen for storage at $-80\text{ }^{\circ}\text{C}$.

The WT PKR protein and mutant (PKR R510Q) used in enzymatic activation assays were purified as described previously and used in thermostability experiments, during which the refolding step was omitted, and the soluble PKR-containing fraction was used for purification after lysis, as previously described.¹⁹

Crystallization, X-ray Data Collection, Processing, Structure Refinement, and Analysis. PKR₅₀₋₅₇₄ (23.0 mg/mL, 20 mM NaCl in PBS, pH 8.0) was incubated with 1 mM compound (100 mM in dimethyl sulfoxide [DMSO]), 5 mM FBP, and 1 mM pyruvate at 4 $^{\circ}\text{C}$ for 2 h. Crystals were obtained by sitting-drop vapor diffusion at 4 $^{\circ}\text{C}$ by mixing 200 nL of protein complex with 180 nL of crystallization well solution and 20 nL of lysozyme seeds, and equilibrating against 60 μL of well solution containing 10 mM MnSO_4 , 50 mM MES/KOH, pH 6.0, and 11% (weight/volume percentage concentration [w/v]) polyethylene glycol 8000. The crystals were cryoprotected in the well solution supplemented with 25% glycerol and flash-frozen in liquid nitrogen. The data for PKR-compound **2** crystal were collected at Shanghai Synchrotron Radiation Facility (SSRF) using beamline BL17U1 with an ADSC Quantum 315r detector, PKR-compound **12** crystal was collected at the SSRF beamline BL19U1 with a Pilatus3 6 M detector, and the PKR-AG-**27** (PKR-AG-946) crystal was collected at the SSRF BL17U1 with the Eiger16M detector. All data were processed with HKL2000 (HKL Research Inc.).²⁰ Initial phases were obtained by performing molecular replacement with the coordinates derived from PDB ID 2VGB as a search template using Phaser in CCP4 Suite.²¹ The restraints and coordinates of the compounds were generated by ProDrG,²² and iterative model building was performed using COOT²³ and refined using REFMAC5 and Phenix.²⁴ The data collection and structure refinement statistics are summarized in Supplementary Table 1. PKR-compound **2** structure contains a tetramer of PKR in the asymmetric unit, with each PKR protein containing FBP and pyruvate. The compound binds at the site between two PKR proteins. PKR₅₀₋₅₇₄-compound **12** and PKR-AG-946 structures contain two tetramers in the asymmetric unit. All figures representing structures were prepared with PyMOL (Schrödinger, Inc.) and MOE (Chemical Computing Group). Atomic coordinates and experimental structure factors have been deposited at the Research Collaboratory for Structural Bioinformatics Protein Data Bank. Deposition codes: 8TBT <https://doi.org/10.2210/pdb8tbt/pdb> for PKR-compound **2**, 8TBU <https://doi.org/10.2210/pdb8tbu/pdb> for PKR-compound **12**, and 8TBS <https://doi.org/10.2210/pdb8tbs/pdb> for PKR-compound **27** complex structures. These data are available free of charge at wwPDB <https://www.wwpdb.org>.

Enzymatic Assay of PK Isoforms and Mutants. Enzymatic activation of WT or mutant PKR enzyme and half-life of activation were measured as described.^[19]

Thermostability Studies. PKR R510Q was mixed with compound and diluted to yield a 10× final concentration of enzyme and a 1× final concentration of compound (10-point 3× serial dilution) in 70 mM MOPS, 140 mM KCl, 7 mM MgCl₂, 1.4 mM dithiothreitol (DTT), 0.007% bovine serum albumin (BSA), and 2% DMSO. After a 60-min incubation period, the enzyme:compound mixture was added to a reaction mixture containing all necessary assay components (see below) preheated to 53 °C. This preheated reaction mixture contained an appropriate amount of compound such that the concentration remained constant when the enzyme:compound mixture was added. Time-dependent changes in absorbance at 340 nm were recorded for 60 min. The final reaction mixture was 0–10 μM compound, 5 mM PEP, 0.4 mM reduced form of nicotinamide adenine dinucleotide (NADH), 2 mM adenosine diphosphate (ADP), 0.45 M Gnd-HCl, 0.00125 U/μL thermostable flavoenzyme dye-linked lactate dehydrogenase (LDH), and 0.12 μg/mL PKR in 1× thermostability reaction buffer.

The rate of conversion (k_{obs}) from the active (v_i) to inactive (v_f) enzyme was measured by fitting the progress curves to equation

$$y = v_f t + \frac{v_i - v_f}{k_{obs}} (1 - e^{-k_{obs} t}) + C.$$

The final rate was non-zero due to non-enzymatic background conversion of NADH to nicotinamide adenine dinucleotide (NAD⁺) under the high-temperature conditions.

Potency of stabilization was derived by plotting k_{obs} vs compound concentration and fitting to a standard sigmoidal four-parameter dose-response equation. Data were analyzed using GraphPad Prism. Magnitude of stabilization experiments were carried out in a manner similar to the standard thermostability experiments, except a single 50 μM compound concentration was used, and the concentration of Gnd-HCl was varied.

Microsome. Human, rat, mouse, dog, and monkey liver microsomes (final concentration of 0.5 mg/mL in 0.1 M potassium phosphate buffer, pH 7.4) were incubated with 1 μM of compound **27** for up to 45 min. Reactions were initiated by the addition of nicotinamide adenine dinucleotide phosphate (NADPH, final concentration 2 mM) to all wells except the 0 min time point. At the end of the incubation period, reactions were stopped by the addition of acetonitrile containing internal standard. For the 0 min time point, acetonitrile containing internal standard was added to the well, followed by NADPH. The assay plates were shaken and then centrifuged at 3,220×g for 10 min to pellet the precipitated protein. The supernatants were diluted with Mill-Q water before being analyzed by liquid chromatography with tandem mass spectrometry (LCMS).

RBC Purification. All biochemistry assays are described in protocol AG-946-N-049 (ChemPartner Study Number CPB<-C->P08-018), and use of tissue samples from human subjects was approved by the ChemPartner institutional ethics committee per protocol number IEC001-R2018 prior to the research. After receiving written informed consent (on file at ChemPartner), fresh whole blood was collected from healthy human volunteers at ChemPartner. Whole blood was centrifuged at 500×g for 10 min. The plasma layer was removed from the centrifuged unit of blood, and the cell pellet was resuspended at 50% hematocrit in PBS. Purified RBCs were isolated from the resuspended cells using a Purecell® Leukocyte Reduction Neofilter. The resuspended cell pellet was transferred to a 10 mL syringe barrel that was attached to the tubing above the filter, and

the cell suspension was allowed to flow through the Purecell Leukocyte Reduction Neofilter. The syringe plunger was inserted into the 10 mL syringe barrel to collect all filtered, purified RBCs in the collection bag. The purified RBCs were centrifuged at 500×g for 10 min at 4 °C and resuspended in a PBS containing 1% glucose, 170 mg/L adenine, and 5.25 g/L mannitol (AGAM) media at a volume equal to that of the starting material.

Cell-based PKR Activity and ATP Assays. Following addition of compound (0.1% final DMSO concentration), cells were incubated at 37 °C overnight. ATP was measured using CellTiter-Glo (Promega, China), while PKR activity was assessed from purified RBC lysate using the LDH-coupled enzyme assay previously described.^[19]

Cell-based PKR Activity Assay. RBCs were diluted in AGAM media to a density of 1×10⁸ cells/mL. Compound **27** (AG-946) serial dilutions were added to 96-well v-bottom plates at 10 μL/well, then purified RBCs (90 mL) were added before the assay plates were covered with aluminum foil seals. All experiments were conducted in triplicate. Plates were incubated at 37 °C in a humidified, non-carbon dioxide (CO₂) chamber for 17–20 h, then washed by centrifugation at 600×g for 5 min, removing 90 μL of supernatant, then adding 200 μL of PBS per well and repeating centrifugation at 600×g for 5 min. Supernatant 200 μL per well was removed and 100 μL of activity assay buffer per well was added. The plates were covered using aluminum foil seals, frozen on dry ice, and stored at –80 °C until assayed for PKR activity. The plates were thawed and RBC lysates were diluted to achieve an optimal concentration for the PKR activity assay by adding 10 μL of RBC lysate to 190 μL of activity assay buffer and mixing well. The PKR protein concentration was determined using a bicinchoninic acid kit. The lysate was further diluted to achieve a concentration range of 1–2 mg/mL by addition of either more RBC lysate or activity assay buffer. Diluted RBC lysate (10–20 μg protein/well) was added to an ultraviolet-transparent 96-well plate at a volume of 10 μL/well. To initiate the reaction, 190 μL master mix (consisting of the following final assay buffer concentrations: 50 mM tris-hydrochloride [HCl], pH 7.5; 100 mM KCl; 5 mM MgCl₂; 0.3 mg/mL BSA; 250 μM NADH; 3 mU/μL LDH; 2 mM ADP; 50 μM PEP) was added to the wells containing the RBC lysate. Plates were read on a SpectraMax® Plus 384 microplate reader (Molecular Devices, LLC) set to kinetic mode (i.e., readings taken every 40 sec for 0.5 h at an absorbance of 340 nm). The PKR activity was determined by evaluating the reaction slope in the linear portion of the reaction (often 2–33 min) and normalizing to the protein concentration of the lysate (final units: μmol/sec/mg of protein).

Cell-based RBC ATP Assay. Purified RBCs were diluted in AGAM media containing 10% fetal bovine serum to a density of 1×10⁷ cells/mL. The compound was serially diluted (0–20,000 nM) and added to 96-well black assay plates at a quantity of 10 μL/well; all experiments were conducted in triplicate. Purified RBCs (90 mL/well) were added to these wells and the assay plates covered using aluminum foil seals. Plates were incubated at 37 °C in a humidified non-CO₂ chamber for 17–20 h, following which 100 μL of CellTiter-Glo was added to each well. Further, each assay plate was placed on an orbital shaker for 30 min and read for luminescence.

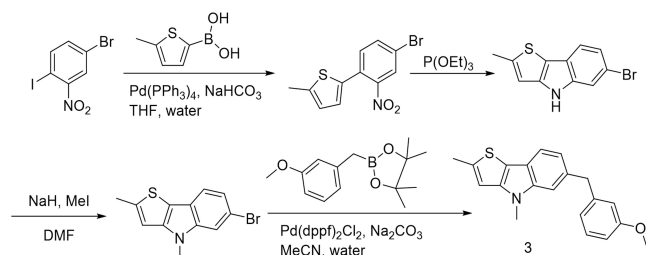
Chemistry

General Experimental Notes. In the following examples, the chemical reagents were purchased from commercial sources (such as Alfa, Acros, Sigma Aldrich, TCI, and Shanghai Chemical Reagent Company) and used without further purification. Flash chromatography was performed on an Ez Purifier III via column chromatography with silica gel particles of 200–300 mesh. Analytic and

preparative thin layer chromatography (prep-TLC) plates were HSGF254 (0.15–0.2 mm thickness, Shanghai Anbang Company, China). Nuclear magnetic resonance (NMR) spectra were recorded using Bruker AMX-300 or AMX-400 NMR (Bruker, Billerica, MA). Chemical shifts were reported in parts per million (δ) downfield from tetramethyl silane. Mass spectra were run with electrospray ionization (ESI) from a Waters LCT TOF Mass Spectrometer (Waters, USA). High-performance liquid chromatography (HPLC) chromatographs were recorded on an Agilent 1200 Liquid Chromatography instrument (Agilent, USA, column: Ultimate 4.6 mm \times 50 mm, 5 mM, mobile phase A: 0.1% formic acid in water; mobile phase B: acetonitrile). Microwave reactions were run on an Initiator 2.5 Microwave Synthesizer (Biotage, Sweden).

Experimental Procedures. Compounds **1** and **2** are literature compounds.

6-(3-methoxybenzyl)-2,4-dimethyl-4H-thieno[3,2-b]indole (3)



NaHCO₃ (257 mg, 3.0 mmol) and Pd(Ph₃P)₄ (140 mg, 0.12 mmol) were added to a mixture of 4-bromo-1-iodo-2-nitrobenzene (400 mg, 1.2 mmol), 5-methylthiophen-2-ylboronic acid (278 mg, 1.9 mmol) in tetrahydrofuran (THF, 8 mL) and water (2 mL). The reaction mixture was stirred at 90 °C for 1 h under a nitrogen atmosphere. The mixture was cooled to room temperature, diluted with water, and extracted with ethyl acetate (EtOAc). The organic layer was dried over anhydrous sodium sulphate (Na₂SO₄) and concentrated. The residue was purified by silica gel chromatography (eluted with petroleum ether (PE):EtOAc = 100:1) to give 2-(4-bromo-2-nitrophenyl)-5-methylthiophene (300 mg, 83% yield).

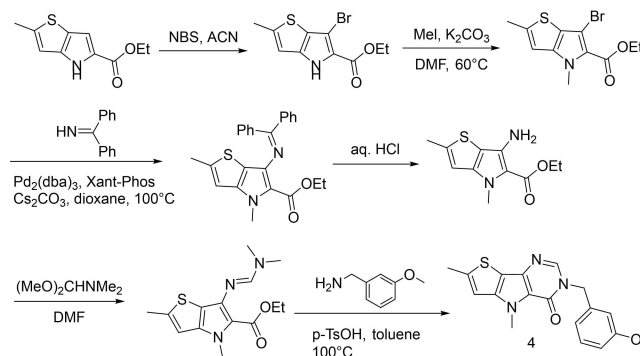
A mixture of 2-(4-bromo-2-nitrophenyl)-5-methylthiophene (300 mg, 1 mmol) in triethyl phosphate (2 mL) was stirred at 170 °C for 2 h. The solvent was removed under reduced pressure and the residue was purified by silica gel chromatography (eluted with PE:EtOAc = 10:1) to give 6-bromo-2-methyl-4H-thieno[3,2-b]indole (260 mg, 98% yield). LCMS (ESI): mass over charge number (m/z) 266 ($M+H$)⁺.

Sodium hydride (80 mg, 2.0 mmol) at 0 °C was added to a solution of 6-bromo-2-methyl-4H-thieno[3,2-b]indole (260 mg, 1.0 mmol) in dimethylformamide (DMF) (5 mL). The mixture was stirred at 0 °C for 15 min. MeI (180 mg, 1.3 mmol) was added and the mixture was stirred at room temperature for another 2 h. The mixture was then poured into saturated NH₄Cl and extracted with EtOAc. The combined organic layer was dried over anhydrous Na₂SO₄ and concentrated. The residue was purified by silica gel chromatography (eluted with PE:EtOAc = 10:1) to give 6-bromo-2,4-dimethyl-4H-thieno[3,2-b]indole (160 mg, 58% yield). LCMS (ESI): m/z 280 ($M+H$)⁺.

Na₂CO₃ (45 mg, 0.42 mmol) and Pd(dppf)₂Cl₂ (11 mg, 0.014 mmol) were added to a mixture of 6-bromo-2,4-dimethyl-4H-thieno[3,2-b]indole (40 mg, 0.14 mmol) and 2-(3-methoxybenzyl)-4,4,5,5-tetramethyl-1,3,2-dioxaborolane (70 mg, 0.28 mmol) in MeCN (8 mL) and water (4 mL). The reaction mixture was stirred at 90 °C for 1 h under a nitrogen atmosphere. The mixture was cooled to room temperature, diluted with water, and extracted with EtOAc.

The organic layer was dried over anhydrous Na₂SO₄ and concentrated. The residue was purified by silica gel chromatography (eluted with PE:EtOAc = 10:1) to give 6-(3-methoxybenzyl)-2,4-dimethyl-4H-thieno[3,2-b]indole (25 mg, 54% yield) as a white solid. LCMS (ESI): m/z 322 ($M+H$)⁺. ¹H NMR (400 MHz, CDCl₃) δ 7.48 (d, 1H), 7.12 (t, 1H), 7.07 (s, 1H), 6.93 (dd, 1H), 6.76 (d, 1H), 6.72–6.64 (m, 3H), 4.04 (s, 2H), 3.70 (s, 3H), 3.69 (s, 3H), 2.56 (d, 3H).

3-(3-methoxybenzyl)-5,7-dimethyl-3H-thieno[2',3':4,5]pyrrolo[3,2-d]pyrimidin-4(5H)-one (4)



N-bromosuccinimide (1 g, 5.7 mmol) was added to a mixture of ethyl 2-methyl-4H-thieno[3,2-b]pyrrole-5-carboxylate (800 mg, 3.8 mmol) in MeCN (10 mL). The mixture was stirred at ambient temperature for 30 min or until the reaction was complete, detected by thin layer chromatography (TLC) (PE:EtOAc = 5:1). The reaction solution was poured into water. The aqueous layer was extracted with EtOAc. The organic layer was concentrated under reduced pressure, and the residue was purified by silica gel chromatography (eluted with PE:ethyl acetate (EA) = 20:1) to give ethyl 6-bromo-2-methyl-4H-thieno[3,2-b]pyrrole-5-carboxylate (400 mg, 40% yield) as a yellow solid. LCMS: 287 ($M+H$)⁺.

Iodomethane (2.93 g, 1.70 mmol) was added to a solution of ethyl 6-bromo-2-methyl-4H-thieno[3,2-b]pyrrole-5-carboxylate (400 mg, 1.40 mmol) and K₂CO₃ (288 mg, 2.10 mmol) in DMF (6 mL). The reaction mixture was stirred at 60 °C for 3 h. TLC (PE:EtOAc = 6:1) showed the reaction was complete. The reaction mixture was poured into water, the aqueous layer was extracted with EtOAc, and the organic layer was concentrated under reduced pressure. The residue was purified by silica gel chromatography (eluted with PE:EtOAc = 30:1) to give ethyl 6-bromo-2,4-dimethyl-4H-thieno[3,2-b]pyrrole-5-carboxylate (300 mg, 72% yield) as a white solid. LCMS: 301 ($M+H$)⁺.

Diphenylmethanimine (490 mg, 2.7 mmol) under nitrogen was added to a mixture of ethyl 6-bromo-2,4-dimethyl-4H-thieno[3,2-b]pyrrole-5-carboxylate (400 mg, 1.30 mmol), Cs₂CO₃ (1.3 g, 4 mmol), and Xant-Phos (150 mg, 0.27 mmol) in dioxane (10 mL). The mixture was stirred at 100 °C overnight and TLC (PE:EtOAc = 6:1) showed the reaction was complete. The reaction mixture was poured into water, the aqueous layer was extracted with EtOAc, and the organic layer was concentrated under reduced pressure. The residue was purified by silica gel chromatography (eluted with PE:EtOAc = 20:1) to give ethyl 6-(diphenylmethylenamino)-2,4-dimethyl-4H-thieno[3,2-b]pyrrole-5-carboxylate (380 mg, 71% yield) as a yellow solid. LCMS: 403 ($M+H$)⁺.

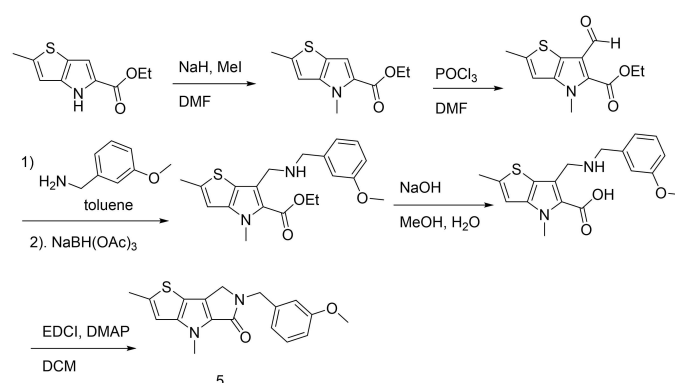
A mixture of ethyl 6-(diphenylmethylenamino)-2,4-dimethyl-4H-thieno[3,2-b]pyrrole-5-carboxylate (200 mg, 0.50 mmol) in 1 M HCl (1 mL) and THF (1 mL) was stirred at ambient temperature for 2 h, and TLC (PE:EtOAc = 3:1) showed the reaction was complete. The reaction mixture was poured into water, the aqueous layer was extracted with EtOAc, and the organic layer was concentrated

under reduced pressure to give ethyl 6-amino-2,4-dimethyl-4H-thieno[3,2-b]pyrrole-5-carboxylate (110 mg, 92% yield) as a yellow oil. LCMS: 239 (M+H)⁺.

Dimethylformamide dimethyl acetal (128 mg, 1.1 mmol) was added to a mixture of ethyl 6-amino-2,4-dimethyl-4H-thieno[3,2-b]pyrrole-5-carboxylate (110 mg, 0.46 mmol) in DMF (5 mL). The mixture was stirred at ambient temperature for 2 h, when TLC (PE:EtOAc = 1:1) showed the reaction was complete. The reaction mixture was poured into water, the aqueous layer was extracted with EtOAc, and the organic layer was concentrated under reduced pressure to give (E)-ethyl 6-((dimethylamino)methyleneamino)-2,4-dimethyl-4H-thieno[3,2-b]pyrrole-5-carboxylate (120 mg, 94% yield) as a yellow oil, which was used without further purification. LCMS: 294 (M+H)⁺.

(3-methoxyphenyl)methanamine (46 mg, 0.27 mmol) was added to a mixture of (E)-ethyl 6-((dimethylamino)methyleneamino)-2,4-dimethyl-4H-thieno[3,2-b]pyrrole-5-carboxylate (80 mg, 0.29 mmol) and TsOH (92 mg, 0.54 mmol) in toluene (3 mL). The mixture was stirred at 100 °C for about 12 h, whereupon TLC (PE:EtOAc = 1:1) showed the reaction was complete. The mixture was concentrated under reduced pressure. The residue was diluted with water and the mixture was extracted with EtOAc. The organic layer was concentrated under reduced pressure, and the residue was purified by silica gel chromatography to give 3-(3-methoxybenzyl)-5,7-dimethyl-3H-thieno[2',3':4,5]pyrrolo[3,2-d]pyrimidin-4(5H)-one (20 mg, 20% yield) as a white solid. ¹H NMR (400 MHz, DMSO-d₆) δ 8.36 (s, 1H), 7.26 (t, *J* = 8.0 Hz, 1H), 7.12 (d, *J* = 1.2 Hz, 1H), 6.93–6.85 (m, 3H), 5.19 (s, 2H), 4.10 (s, 3H), 3.74 (s, 3H), 2.60 (d, *J* = 0.8 Hz, 3H). LCMS: 340 (M+H)⁺.

6-(3-methoxybenzyl)-2,4-dimethyl-6,7-dihydropyrrolo[3,4-b]thieno[2,3-d]pyrrol-5(4H)-one (5)



NaH (114 mg, 4.8 mmol) at 0 °C was added to a mixture of ethyl 2-methyl-4H-thieno[3,2-b]pyrrole-5-carboxylate (500 mg, 2.4 mmol) in DMF (30 mL). The mixture was stirred at room temperature for 30 min, followed by the addition of MeI (678 mg, 4.78 mmol) at 0 °C. After stirring at room temperature for 2 h, the mixture was poured into saturated NH₄Cl and extracted with EtOAc. The combined organic layer was dried over anhydrous Na₂SO₄ and concentrated. The residue was purified by silica gel chromatography to give ethyl 2,4-dimethyl-4H-thieno[3,2-b]pyrrole-5-carboxylate (420 mg, 79% yield) as a yellow solid. LCMS (ESI): *m/z* 224 (M+H)⁺.

POCl₃ (618 mg, 4.0 mmol) at 0 °C was added to a mixture of ethyl 2,4-dimethyl-4H-thieno[3,2-b]pyrrole-5-carboxylate (300 mg, 1.3 mmol) in anhydrous DMF (15 mL). The mixture was stirred at 90 °C overnight, then cooled to room temperature, poured into ice water, neutralized with ammonia, and extracted with EtOAc. The combined organic layers were dried over anhydrous Na₂SO₄ and concentrated. The

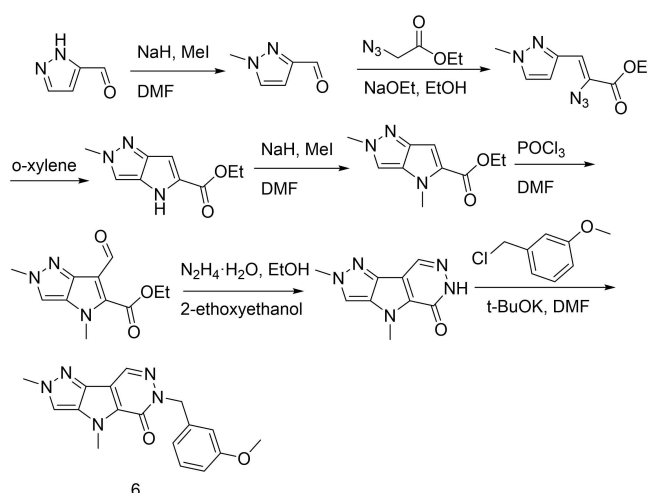
residue was purified by silica gel chromatography to give ethyl 6-formyl-2,4-dimethyl-4H-thieno[3,2-b]pyrrole-5-carboxylate (250 mg, 74% yield) as a yellow solid. LCMS (ESI): *m/z* 252 (M+H)⁺.

A mixture of ethyl 6-formyl-2,4-dimethyl-4H-thieno[3,2-b]pyrrole-5-carboxylate (150 mg, 0.6 mmol) and (3-methoxyphenyl)methanamine (98 mg, 0.7 mmol) in toluene (20 mL) was stirred at 60 °C for 2 h. NaBH(OAc)₃ (380 mg, 1.8 mmol) was then added at 0 °C and stirred at room temperature overnight. The mixture was poured into water and extracted with EtOAc. The organic layer was dried over anhydrous Na₂SO₄ and concentrated. The residue was purified by silica gel chromatography to give ethyl 6-(((3-methoxybenzyl)amino)methyl)-2,4-dimethyl-4H-thieno[3,2-b]pyrrole-5-carboxylate (80 mg, 36% yield) as a white solid. LCMS (ESI): *m/z* 373 (M+H)⁺.

NaOH (16 mg, 0.4 mmol) was added to a mixture of 6-(((3-methoxybenzyl)amino)methyl)-2,4-dimethyl-4H-thieno[3,2-b]pyrrole-5-carboxylate (50 mg, 0.13 mmol) in MeOH (5 mL) and H₂O (5 mL). The mixture was stirred at 30 °C overnight, acidified to pH = 3 with aqueous HCl, and extracted with dichloromethane (DCM). The organic layer was dried over anhydrous Na₂SO₄ and concentrated to give 6-(((3-methoxybenzyl)amino)methyl)-2,4-dimethyl-4H-thieno[3,2-b]pyrrole-5-carboxylic acid (50 mg, 100% yield) as a white solid, which was used directly in the next step. LCMS (ESI): *m/z* 345 (M+H)⁺.

4-dimethylaminopyridine (DMAP) (35 mg, 0.3 mmol) and 1-ethyl-3-(3-dimethylaminopropyl)carbodiimide (EDCI) (55 mg, 0.3 mmol) were added to a mixture of 6-(((3-methoxybenzyl)amino)methyl)-2,4-dimethyl-4H-thieno[3,2-b]pyrrole-5-carboxylic acid (50 mg, 0.15 mmol) in DCM (10 mL). After stirring at 30 °C overnight, the reaction mixture was poured into water and extracted with EtOAc. The organic layer was dried over anhydrous Na₂SO₄ and concentrated. The residue was purified by prep-TLC to give 6-(3-methoxybenzyl)-2,4-dimethyl-6,7-dihydropyrrolo[3,4-b]thieno[2,3-d]pyrrol-5(4H)-one (16 mg, 34% yield) as a white solid. LCMS (ESI): *m/z* 327 (M+H)⁺. ¹H NMR (400 MHz, DMSO-d₆) δ 7.25 (t, 1H), 6.98 (s, 1H), 6.79–6.86 (m, 3H), 4.59 (s, 2H), 4.18 (s, 2H), 3.86 (s, 3H), 3.73 (s, 3H), 2.51 (s, 3H).

6-(3-methoxybenzyl)-2,4-dimethyl-4,6-dihydropyrazolo[3',4':4,5]pyrrolo[2,3-d]pyridazin-5(2H)-one (6)



NaH (4.3 g, 108 mmol) and iodomethane (1.15 g, 81 mmol) were added to a solution of 1H-pyrazole-3-carbaldehyde (5.2 g, 54 mmol) in DMF (30 mL). The mixture was stirred at room temperature for 2 h. The reaction mixture was poured into saturated NH₄Cl and extracted with EtOAc. The organic phase was washed with brine,

dried over anhydrous Na_2SO_4 , filtered, and concentrated. The residue was purified by silica gel chromatography (eluted with PE:EtOAc = 20:1) to obtain 1-methyl-1H-pyrazole-3-carbaldehyde (4.18 g, 70% yield) as a white solid. LCMS (ESI): m/z 111 ($M+H$)⁺.

1-methyl-1H-pyrazole-3-carbaldehyde (1.0 g, 9.2 mmol) and azidoacetic acid ethyl ester (1.3 g, 10.1 mmol) at -10°C were added to a solution of sodium ethoxide (EtONa) (1.8 g, 18.4 mmol) in ethanol (EtOH) (20 mL). After stirring for 3 h, the reaction mixture was poured into saturated NH_4Cl and extracted with EtOAc. The organic phase was washed with brine, dried over anhydrous Na_2SO_4 , filtered, and concentrated. The residue was purified by silica gel chromatography (eluted with PE:EtOAc = 10:1) to obtain (Z)-ethyl 2-azido-3-(1-methyl-1H-pyrazol-3-yl)acrylate (0.77 g, 38% yield) as a white solid. LCMS (ESI): m/z 222 ($M+H$)⁺.

A mixture of (Z)-ethyl 2-azido-3-(1-methyl-1H-pyrazol-3-yl)acrylate (0.77 g, 3.5 mmol) in *o*-xylene (15 mL) was heated to reflux for 2 h. The reaction mixture was concentrated and the residue was purified by silica gel chromatography (eluted with PE:EtOAc = 5:1) to obtain ethyl 2-methyl-2,4-dihydropyrrolo[3,2-c]pyrazole-5-carboxylate (500 mg, 82% yield) as a white solid. LCMS (ESI): m/z 194 ($M+H$)⁺.

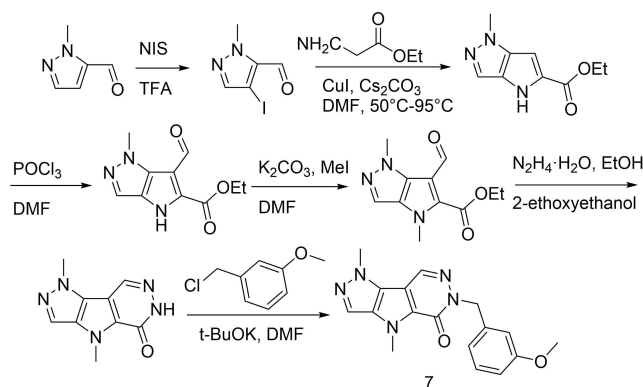
NaH (207 mg, 5.2 mmol) and iodomethane (552 mg, 3.9 mmol) were added to a solution of ethyl 2-methyl-2,4-dihydropyrrolo[3,2-c]pyrazole-5-carboxylate (500 mg, 2.6 mmol) in DMF (10 mL). The mixture was stirred at room temperature for 2 h, poured into saturated NH_4Cl , and extracted with EtOAc. The organic phase was washed with brine, dried over anhydrous Na_2SO_4 , filtered, and concentrated. The residue was purified by silica gel chromatography (eluted with PE:EtOAc = 15:1) to obtain ethyl 2,4-dimethyl-2,4-dihydropyrrolo[3,2-c]pyrazole-5-carboxylate (500 mg, 93% yield) as a white solid. LCMS (ESI): m/z 208 ($M+H$)⁺.

POCl_3 (1.85 g, 12.1 mmol) was added to a mixture of ethyl 2,4-dimethyl-2,4-dihydropyrrolo[3,2-c]pyrazole-5-carboxylate (500 mg, 2.4 mmol) in DMF (10 mL). The reaction mixture was stirred at 90°C for 3 h, poured into water, and extracted with EtOAc. The organic phase was washed with brine, dried over anhydrous Na_2SO_4 , filtered, and concentrated. The residue was purified by silica gel chromatography (eluted with PE:EtOAc = 15:1) to obtain ethyl 6-formyl-2,4-dimethyl-2,4-dihydropyrrolo[3,2-c]pyrazole-5-carboxylate (150 mg, 26% yield) as a white solid. LCMS (ESI): m/z 236 ($M+H$)⁺.

$\text{N}_2\text{H}_4\cdot\text{H}_2\text{O}$ (319 mg, 6.4 mmol) was added to a solution of ethyl 6-formyl-2,4-dimethyl-2,4-dihydropyrrolo[3,2-c]pyrazole-5-carboxylate (150 mg, 0.64 mmol) in 2-ethoxyethanol (5 mL). The reaction mixture was stirred at 100°C for 2 h, poured into water, and extracted with EtOAc. The organic phase was washed with brine, dried over anhydrous Na_2SO_4 , filtered, and concentrated. The residue was purified by silica gel chromatography (eluted with PE:EtOAc = 3:1) to obtain 2,4-dimethyl-4,6-dihydropyrrolo[3',4':4,5]pyrrolo[2,3-d]pyridazin-5(2H)-one (120 mg, 92% yield) as a white solid. LCMS (ESI): m/z 204 ($M+H$)⁺.

t-BuOK (33 mg, 0.3 mmol) and 1-chloromethyl-3-methoxybenzene (46 mg, 0.3 mmol) were added to a solution of 2,4-dimethyl-4,6-dihydropyrrolo[3',4':4,5]pyrrolo[2,3-d]pyridazin-5(2H)-one (30 mg, 0.15 mmol) in DMF (3 mL). The mixture was stirred at room temperature for 2 h. The reaction mixture was poured into saturated NH_4Cl and extracted with EtOAc. The organic phase was washed with brine, dried over anhydrous Na_2SO_4 , filtered, and concentrated. The residue was purified by prep-TLC (EtOAc:PE = 3:1) to obtain 6-(3-methoxybenzyl)-2,4-dimethyl-4,6-dihydropyrrolo[3',4':4,5]pyrrolo[2,3-d]pyridazin-5(2H)-one (10 mg, 26% yield) as a white solid. LCMS (ESI): m/z 324 ($M+H$)⁺. ¹H NMR (400 MHz, $\text{DMSO}-d_6$) δ 8.47 (s, 1H), 8.02 (s, 1H), 7.24 (t, 1H), 6.82–6.89 (m, 3H), 5.33 (s, 2H), 4.12 (s, 3H), 4.11 (s, 3H), 3.72 (s, 3H).

6-(3-methoxybenzyl)-1,4-dimethyl-4,6-dihydropyrrolo[3',4':4,5]pyrrolo[2,3-d]pyridazin-5(1H)-one (7)



NIS (3.4 g, 15 mmol) was added at 0°C to a stirred mixture of 1-methyl-1H-pyrazole-5-carbaldehyde (1.1 g, 10 mmol) in trifluoroacetic acid (TFA; 10 mL). After stirring at room temperature for 16 h, the reaction mixture was poured into saturated NaHCO_3 and extracted with DCM. The organic layer was dried over anhydrous Na_2SO_4 and concentrated. The residue was purified by silica gel chromatography (eluted with PE:EtOAc = 35:1) to obtain 4-iodo-1-methyl-1H-pyrazole-5-carbaldehyde (1.8 g, 76% yield) as a white solid. LCMS (ESI): m/z 237 ($M+H$)⁺.

Cs_2CO_3 (274 mg, 0.84 mmol), ethyl 2-isocynoacetate (53 mg, 0.47 mmol) and CuI (15 mg, 0.08 mmol) were added to a stirred mixture of 4-iodo-1-methyl-1H-pyrazole-5-carbaldehyde (100 mg, 0.42 mmol) in DMF (10 mL). The reaction mixture was stirred under N_2 at 50°C for 1 h and 95°C for 16 h. The reaction mixture was poured into water and extracted with EtOAc. The organic layer was dried over anhydrous Na_2SO_4 and concentrated. The residue was purified by silica gel chromatography (eluted with DCM:MeOH = 35:1) to obtain ethyl 1-methyl-1,4-dihydropyrrolo[3,2-c]pyrazole-5-carboxylate (40 mg, 50% yield) as a white solid. LCMS (ESI): m/z 194 ($M+H$)⁺.

POCl_3 (230 mg, 1.5 mmol) was added dropwise at 0°C to a stirred mixture of ethyl 1-methyl-1,4-dihydropyrrolo[3,2-c]pyrazole-5-carboxylate (193 mg, 1 mmol) in dry DMF (5 mL). The reaction mixture was stirred at 100°C under N_2 for 3 h and then cooled down. The reaction mixture was poured into water and extracted with DCM. The organic layer was dried over anhydrous Na_2SO_4 and concentrated to obtain ethyl 6-formyl-1-methyl-1,4-dihydropyrrolo[3,2-c]pyrazole-5-carboxylate (180 mg, 86% yield) as a white solid. LCMS (ESI): m/z 222 ($M+H$)⁺.

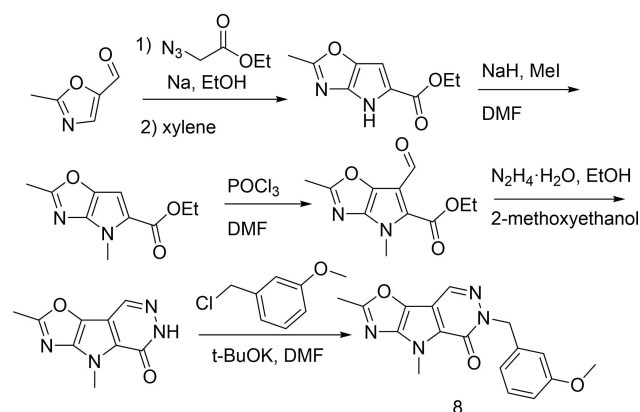
K_2CO_3 (276 mg, 2 mmol) and MeI (280 mg, 2 mmol) were added to a stirred mixture of ethyl 6-formyl-1-methyl-1,4-dihydropyrrolo[3,2-c]pyrazole-5-carboxylate (220 mg, 1 mmol) in dry DMF (5 mL). After stirring at room temperature overnight, the reaction mixture was poured into saturated NH_4Cl and extracted with EtOAc. The organic layer was dried over anhydrous Na_2SO_4 and concentrated. The residue was purified by silica gel chromatography (eluted with PE:EtOAc = 15:1) to obtain ethyl 6-formyl-1,4-dimethyl-1,4-dihydropyrrolo[3,2-c]pyrazole-5-carboxylate (200 mg, 87% yield) as a white solid. LCMS (ESI): m/z 236 ($M+H$)⁺.

$\text{N}_2\text{H}_4\cdot\text{H}_2\text{O}$ (200 mg, 4 mmol, 98% weight by weight [w/w]) was added to a stirred mixture of ethyl 6-formyl-1,4-dimethyl-1,4-dihydropyrrolo[3,2-c]pyrazole-5-carboxylate (470 mg, 2 mmol) in 2-methoxyethanol (5 mL). The reaction mixture was stirred at 105°C for 3 h, diluted with water, and extracted with DCM. The organic phase was washed with brine, dried over anhydrous Na_2SO_4 , and concentrated to obtain 1,4-dimethyl-4,6-dihydropyrrolo-

[3',4':4,5]pyrrolo[2,3-d]pyridazin-5(1H)-one (400 mg, 98% yield) as a white solid. LCMS (ESI): m/z 204 ($M+H$)⁺.

t-BuOK (224 mg, 2.0 mmol) and 1-(chloromethyl)-3-methoxybenzene (312 mg, 2 mmol) were added to a stirred mixture of 1,4-dimethyl-4,6-dihydropyrazolo[3',4':4,5]pyrrolo[2,3-d]pyridazin-5(1H)-one (203 mg, 1.0 mmol) in DMF (4 mL). The reaction mixture was stirred at room temperature for 2 h. The reaction mixture was poured into saturated NH₄Cl and extracted with DCM. The organic layer was dried over anhydrous Na₂SO₄ and concentrated. The residue was purified by silica gel chromatography (eluted with DCM:MeOH = 30:1) to obtain 6-(3-methoxybenzyl)-1,4-dimethyl-4,6-dihydropyrazolo[3',4':4,5]pyrrolo[2,3-d]pyridazin-5(1H)-one (30 mg, 9% yield) as a white solid. LCMS (ESI): m/z 324 ($M+H$)⁺. ¹H NMR (400 MHz, DMSO-*d*₆) δ 8.64 (s, 1H), 7.74 (s, 1H), 7.24 (t, 1H), 6.88–6.80 (m, 3H), 5.33 (s, 2H), 4.16 (s, 3H), 4.13 (s, 3H), 3.72 (s, 3H).

6-(3-methoxybenzyl)-2,4-dimethyl-4,6-dihydro-5H-oxazolo[5',4':4,5]pyrrolo[2,3-d]pyridazin-5-one (8)



A mixture of 2-methyloxazole-5-carbaldehyde (1.0 g, 9.0 mmol) and ethyl 2-azidoacetate (3.4 g, 27 mmol) was added at -10°C over 1 h to a solution of Na (0.65 g, 27 mmol) in dry EtOH (10 mL). The reaction mixture was stirred at 5°C for another hour, then quenched with saturated NH₄Cl and extracted with EtOAc. The combined organic layer was dried over anhydrous Na₂SO₄ and concentrated to give ethyl 2-azido-3-(2-methyloxazol-5-yl)acrylate (1.1 g crude).

A solution of ethyl 2-azido-3-(2-methyloxazol-5-yl)acrylate (1.1 g) in xylene (30 mL) was stirred at 160°C for 30 min and concentrated under reduced pressure. The residue was purified by silica gel chromatography to give ethyl 2-methyl-4H-pyrrolo[2,3-d]oxazole-5-carboxylate (0.25 g, 15% yield). LCMS (ESI): m/z 195 ($M+H$)⁺.

NaH (104 mg, 2.6 mmol) was added at 0°C to a solution of ethyl 2-methyl-4H-pyrrolo[2,3-d]oxazole-5-carboxylate (0.25 g, 1.3 mmol) in DMF (10 mL). The mixture was stirred at 0°C for 15 min. MeI (0.23 g, 1.7 mmol) was added, and the mixture was stirred at room temperature for 2 h, poured into saturated NH₄Cl, and extracted with EtOAc. The combined organic layer was dried over anhydrous Na₂SO₄ and concentrated. The residue was purified by silica gel chromatography to give ethyl 2,4-dimethyl-4H-pyrrolo[2,3-d]oxazole-5-carboxylate (0.2 g, 70% yield). LCMS (ESI): m/z 209 ($M+H$)⁺.

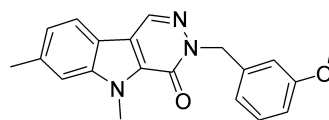
A solution of ethyl 2,4-dimethyl-4H-pyrrolo[2,3-d]oxazole-5-carboxylate (0.2 g, 1.0 mmol) and POCl₃ (0.3 g, 2.0 mmol) in DMF (10 mL) was stirred at 100°C overnight. The reaction mixture was poured into saturated NaHCO₃ and extracted with EtOAc. The combined organic layers were dried over anhydrous Na₂SO₄ and concentrated. The residue was purified by silica gel chromatography to give ethyl 6-formyl-2,4-dimethyl-4H-pyrrolo[2,3-d]-

oxazole-5-carboxylate (100 mg, 45% yield). LCMS (ESI): m/z 237 ($M+H$)⁺.

N₂H₄·H₂O (100 mg, 2.0 mmol) was added to a solution of ethyl 6-formyl-2,4-dimethyl-4H-pyrrolo[2,3-d]oxazole-5-carboxylate (100 mg, 0.42 mmol) in 2-methoxyethanol (15 mL). The solution was stirred at 100°C overnight and concentrated under reduced pressure. The residue was purified by prep-TLC to give 2,4-dimethyl-4,6-dihydro-5H-oxazolo[5',4':4,5]pyrrolo[2,3-d]pyridazin-5-one (50 mg, 50% yield). LCMS (ESI): m/z 205 ($M+H$)⁺.

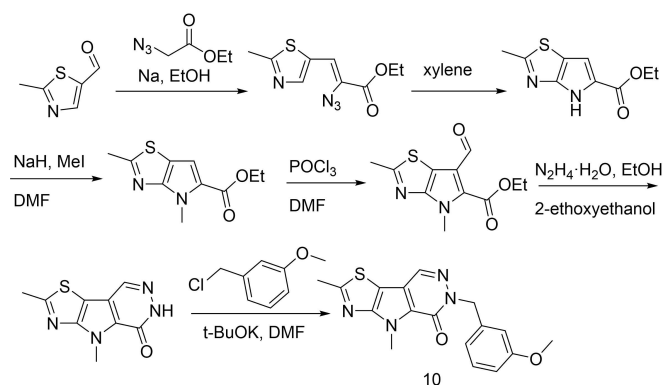
t-BuOK (40 mg, 0.34 mmol) under N₂ was added at 0°C to a solution of 2,4-dimethyl-4,6-dihydro-5H-oxazolo[5',4':4,5]pyrrolo[2,3-d]pyridazin-5-one (50 mg, 0.23 mmol) in DMF (5 mL). The mixture was stirred at 0°C for 20 min, then 1-(chloromethyl)-3-methoxybenzene (40 mg, 0.3 mmol) was added and the mixture was stirred at room temperature for another 2 h. The mixture was poured into saturated NH₄Cl and extracted with EtOAc. The combined organic layers were dried over anhydrous Na₂SO₄ and concentrated. The residue was purified by prep-HPLC to give 6-(3-methoxybenzyl)-2,4-dimethyl-4,6-dihydro-5H-oxazolo[5',4':4,5]pyrrolo[2,3-d]pyridazin-5-one (2 mg, 3% yield). LCMS (ESI): m/z 325 ($M+H$)⁺. ¹H NMR (400 MHz, CDCl₃) δ 8.14 (s, 1H), 7.14–7.19 (m, 1H), 6.91–6.95 (m, 1H), 6.89 (s, 1H), 6.73 (dd, 1H), 5.33 (s, 2H), 4.20 (s, 3H), 3.71 (s, 3H), 2.61 (s, 3H).

3-(3-methoxybenzyl)-5,8-dimethyl-3,5-dihydro-4H-pyridazino[4,5-b]indol-4-one (9)



LCMS: m/z 334 ($M+H$)⁺. ¹H NMR (400 MHz, DMSO-*d*₆) δ 8.77 (s, 1H), 7.99 (s, 1H), 7.65 (d, $J=8.6$ Hz, 1H), 7.43 (dt, $J=10.5, 5.2$ Hz, 1H), 7.24 (t, $J=7.8$ Hz, 1H), 6.88–6.83 (m, 3H), 5.35 (s, 2H), 4.26 (s, 3H), 3.72 (s, 3H), 2.49 (s, 3H).

6-(3-methoxybenzyl)-2,4-dimethyl-4,6-dihydro-5H-thiazolo[5',4':4,5]pyrrolo[2,3-d]pyridazin-5-one (10)



A solution of 2-methylthiazole-5-carbaldehyde (500 mg, 3.93 mmol) and ethyl 2-azidoacetate (1.53 g, 11.79 mmol) in anhydrous EtOH (3 mL) was added dropwise to a solution of EtONa (803 mg, 11.79 mmol) in EtOH (10 mL) at approximately -10°C to -5°C . The reaction mixture was stirred for approximately 1 h while the temperature was maintained below 0°C , then warmed to room temperature and stirred for another 2 h. The resulting mixture was poured into saturated aqueous NH₄Cl (50 mL) at 0°C and extracted with EtOAc. The combined organic layers were washed with brine, dried over anhydrous Na₂SO₄, and concentrated under reduced pressure to give

the desired product (500 mg), which was directly used in the next step without any purification. LCMS: m/z 239 ($M+H$)⁺.

A mixture of ethyl (Z)-2-azido-3-(2-methylthiazol-5-yl)acrylate (500 mg, 2.1 mmol) in *o*-xylene (5 mL) was stirred at 140 °C for 2 h, then cooled to room temperature and directly purified by column chromatography on silica gel (eluent: pentane/EtOAc=6/1) to give the desired product (220 mg, 49.8% yield) as a white solid. LCMS: m/z 211 ($M+H$)⁺.

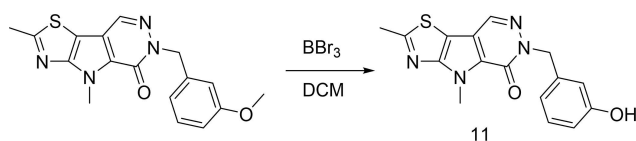
NaH (36.5 mg, 1.52 mmol) was added to a solution of ethyl 2-methyl-4H-pyrrolo[2,3-d]thiazole-5-carboxylate (160 mg, 0.76 mmol) in DMF (3 mL) at 0 °C. The reaction mixture was stirred at room temperature for 0.5 h, followed by the addition of CH₃I (47 μL, 0.76 mmol). The resulting mixture was stirred at room temperature for 0.5 h, then poured into saturated aqueous NH₄Cl at 0 °C and extracted with EtOAc. The combined organic layers were washed with brine, dried over anhydrous Na₂SO₄, and concentrated under reduced pressure. The residue was purified by column chromatography on silica gel (eluent: pentane/EtOAc=6/1) to give the desired product (124 mg, 72.6% yield) as a white solid. LCMS: m/z 225 ($M+H$)⁺.

POCl₃ (122.5 μL, 1.338 mmol) was added to a mixture of ethyl 2,4-dimethyl-4H-pyrrolo[2,3-d]thiazole-5-carboxylate (100 mg, 0.446 mmol) in DMF (1 mL) at 0 °C. The reaction mixture was stirred at 100 °C for 2 h, poured into saturated aqueous NaHCO₃ at 0 °C, and extracted with EtOAc. The combined organic layers were washed with brine, dried over anhydrous Na₂SO₄, and concentrated under reduced pressure. The residue was purified by column chromatography on silica gel (eluent: pentane/EtOAc=5/1) to give the desired product (57 mg, 50.7% yield) as a white solid. LCMS: m/z 253 ($M+H$)⁺.

N₂H₄·H₂O (53.7 μL, 1.130 mmol) was added to a mixture of ethyl 6-formyl-2,4-dimethyl-4H-pyrrolo[2,3-d]thiazole-5-carboxylate (57 mg, 0.226 mmol) in 2-ethoxyethanol (2 mL). The reaction mixture was stirred at 100 °C for 1 h, then poured into H₂O and extracted with EtOAc. The combined organic layers were washed with brine, dried over anhydrous Na₂SO₄, and concentrated under reduced pressure. The residue was purified by column chromatography on silica gel (eluent: pentane/EtOAc=5/1) to give the desired product (49 mg, 98.4% yield) as a white solid. LCMS: m/z 221 ($M+H$)⁺.

t-BuOK (50.8 mg, 0.454 mmol) was added to a mixture of 2,4-dimethyl-4,6-dihydro-5H-thiazolo[5',4':4,5]pyrrolo[2,3-d]pyridazin-5-one (49 mg, 0.223 mmol) in DMF (1 mL) at 0 °C. The reaction mixture was stirred at room temperature for 0.5 h, followed by addition of 1-(chloromethyl)-3-methoxybenzene (34.9 mg, 0.223 mmol). The resulting mixture was stirred at room temperature for 1 h, then poured into saturated aqueous NH₄Cl solution at 0 °C and extracted with EtOAc. The combined organic layers were washed with brine, dried over anhydrous Na₂SO₄, and concentrated under reduced pressure. The residue was purified by column chromatography on silica gel (eluent: pentane/EtOAc=3/1) to give 8 mg of the desired product 6-(3-methoxybenzyl)-2,4-dimethyl-4,6-dihydro-5H-thiazolo[5',4':4,5]pyrrolo[2,3-d]pyridazin-5-one. LCMS: m/z 341 ($M+H$)⁺. ¹H NMR (400 MHz, DMSO-*d*₆) δ 8.56 (s, 1H), 7.23 (t, *J*=7.9 Hz, 1H), 6.92–6.72 (m, 3H), 5.32 (s, 2H), 4.26 (s, 3H), 3.72 (s, 3H), 2.85 (s, 3H).

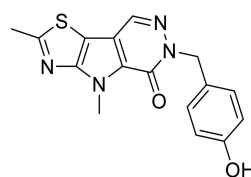
6-(3-hydroxybenzyl)-2,4-dimethyl-4H-thiazolo[5',4':4,5]pyrrolo[2,3-d]pyridazin-5(6H)-one (11)



BBr₃ (195 mg, 0.778 mmol) was added to a mixture of 6-(3-methoxybenzyl)-2,4-dimethyl-4H-thiazolo[5',4':4,5]pyrrolo[2,3-d]pyridazin-5(6H)-one (53 mg, 0.16 mmol) in DCM (4 mL) at 0 °C. The mixture was stirred at room temperature for 2 h and then quenched with MeOH. The resulting mixture was concentrated under reduced pressure. The residue was purified by prep-HPLC to give the desired product (15.6 mg, 30.7% yield) as a white solid. LCMS: m/z 327 ($M+H$)⁺. ¹H NMR (400 MHz, DMSO-*d*₆) δ 9.34 (s, 1H), 8.58 (s, 1H), 7.12 (t, *J*=7.8 Hz, 1H), 6.78–6.56 (m, 3H), 5.26 (s, 2H), 4.278 (s, 3H), 2.86 (s, 3H).

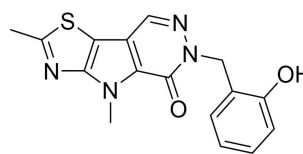
Compounds **12** and **13** were made using a similar procedure as that used for making compound **11**.

6-(4-hydroxybenzyl)-2,4-dimethyl-4,6-dihydro-5H-thiazolo[5',4':4,5]pyrrolo[2,3-d]pyridazin-5-one (12)



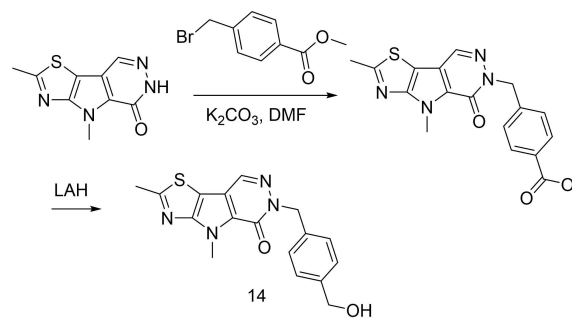
LCMS: 327 ($M+H$)⁺. ¹H NMR (400 MHz, DMSO-*d*₆) δ 9.36 (s, 1H), 8.53 (s, 1H), 7.17 (d, *J*=8.4 Hz, 2H), 6.70 (d, *J*=8.6 Hz, 2H), 5.22 (s, 2H), 4.26 (s, 3H), 2.85 (s, 3H).

6-(2-hydroxybenzyl)-2,4-dimethyl-4,6-dihydro-5H-thiazolo[5',4':4,5]pyrrolo[2,3-d]pyridazin-5-one (13)



LCMS: m/z 327 ($M+H$)⁺. ¹H NMR (400 MHz, DMSO-*d*₆) δ 9.67 (s, 1H), 8.59 (s, 1H), 7.07 (d, *J*=9.1 Hz, 1H), 6.85 (s, 2H), 6.70 (s, 1H), 5.32 (s, 2H), 4.27 (s, 3H), 2.87 (s, 3H).

6-(4-(hydroxymethyl)benzyl)-2,4-dimethyl-4,6-dihydro-5H-thiazolo[5',4':4,5]pyrrolo[2,3-d]pyridazin-5-one (14)

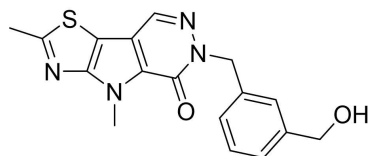


K₂CO₃ (181 mg, 1.3 mmol) was added to a mixture of 2,4-dimethyl-4H-thiazolo[5',4':4,5]pyrrolo[2,3-d]pyridazin-5(6H)-one (100 mg, 0.4 mmol) in DMF (20 mL). The mixture was stirred at 60 °C for 30 min, followed by addition of methyl 4-(bromomethyl)benzoate (100 mg, 0.4 mmol) at 0 °C. The resulting mixture was stirred at 60 °C for 18 h, then poured into ice water and extracted with EtOAc. The combined organic layers were washed with brine, dried over anhydrous Na₂SO₄, and concentrated under reduced pressure. The residue was purified by column chromatography on silica gel (eluent: PE/EtOAc=50/1 to 10/1) to give the desired product (120 mg, 74.61% yield) as a white solid. LCMS: m/z 369 ($M+H$)⁺.

LAH (30 mg, 0.8 mmol) was added to a mixture of methyl 4-((2,4-dimethyl-5-oxo-4H-thiazolo[5',4':4,5]pyrrolo[2,3-d]pyridazin-5H-yl)methyl)benzoate (100 mg, 0.3 mmol) in THF (20 mL) at 0 °C. The resulting mixture was stirred at 0 °C under N₂ for 30 min, and then quenched with Na₂SO₄·10H₂O and filtered. The filtrate was concentrated under reduced pressure. The residue was purified by prep-TLC to give the desired product (3 mg, 3.25% yield) as a white solid. LCMS: m/z 341 (M+H)⁺. ¹H NMR (400 MHz, CDCl₃) δ 8.12 (s, 1H), 7.37 (d, J=8.0 Hz, 2H), 7.25 (d, J=8.0 Hz, 2H), 5.37 (s, 2H), 4.66–4.54 (m, 2H), 4.31 (s, 3H), 2.82 (d, J=10.3 Hz, 3H).

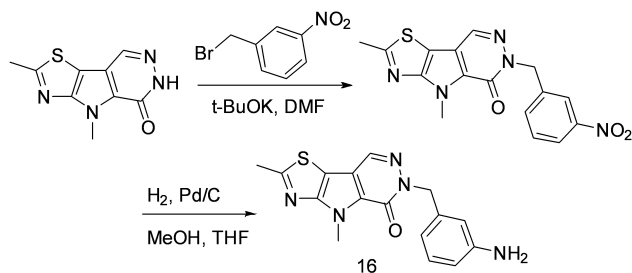
Compound **15** was made utilizing the above procedure, except with methyl 3-(bromomethyl)benzoate.

6-(3-(hydroxymethyl)benzyl)-2,4-dimethyl-4,6-dihydro-5H-thiazolo[5',4':4,5]pyrrolo[2,3-d]pyridazin-5-one (15)



LCMS: m/z 341 (M+H)⁺. ¹H NMR (400 MHz, CDCl₃) δ 8.22 (s, 1H), 7.44 (s, 1H), 7.40–7.29 (m, 3H), 5.47 (s, 2H), 4.69 (s, 2H), 4.39 (d, J=11.0 Hz, 3H), 2.90 (s, 3H).

6-(3-aminobenzyl)-2,4-dimethyl-4H-thiazolo[5',4':4,5]pyrrolo [2,3-d]pyridazin-5(6H)-one (16)

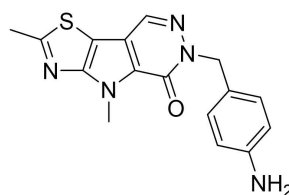


1-(bromomethyl)-3-nitrobenzene (194 mg, 0.9 mmol) and t-BuOK (76 mg, 0.68 mmol) were added to a mixture of 2,4-dimethyl-4H-thiazolo[5',4':4,5]pyrrolo[2,3-d]pyridazin-5(6H)-one (100 mg, 0.45 mmol) in DMF (5 mL). The resulting mixture was stirred at room temperature for 1 h, then poured into water and extracted with EtOAc. The combined organic layers were washed with brine, dried over anhydrous Na₂SO₄, and concentrated under reduced pressure. The residue was purified by prep-TLC to give the desired product (100 mg, 62.5% yield). LCMS: m/z 356 (M+H)⁺.

Pd/C (10%, 50 mg) was added to a mixture of 2,4-dimethyl-6-(3-nitrobenzyl)-4H-thiazolo[5',4':4,5]pyrrolo[2,3-d]pyridazin-5(6H)-one (100 mg, 0.28 mmol) in MeOH/THF (10 mL/10 mL) under N₂. The reaction mixture was stirred at 40 °C under H₂ for 12 h and then filtered through Celite. The filtrate was concentrated under reduced pressure and the residue was purified by prep-TLC to obtain the desired compound (80 mg, 88% yield). LCMS: m/z 326 (M+H)⁺. ¹H NMR (400 MHz, DMSO-d₆) δ 8.54 (s, 1H), 6.94 (t, 1H), 6.57–6.32 (m, 3H), 5.19 (s, 2H), 5.04 (s, 2H), 4.26 (s, 3H), 2.85 (s, 3H).

Compound **17** was made utilizing the above procedure.

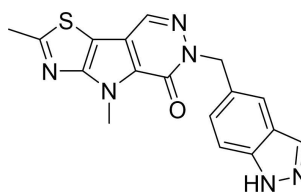
6-(4-aminobenzyl)-2,4-dimethyl-4,6-dihydro-5H-thiazolo[5',4':4,5]pyrrolo[2,3-d]pyridazin-5-one (17)



LCMS: m/z 326 (M+H)⁺. ¹H NMR (400 MHz, DMSO-d₆) δ 8.52 (s, 1H), 7.04 (d, 2H), 6.49 (d, 2H), 5.15 (s, 2H), 5.01 (s, 2H), 4.25 (s, 3H), 2.85 (s, 3H).

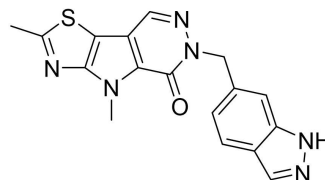
Compounds **18–21** and the 6-fluoropyridin-2-ylmethyl analog were all made using 2,4-dimethyl-4H-thiazolo[5',4':4,5]pyrrolo[2,3-d]pyridazin-5(6H)-one and corresponding benzylic halides in one step.

6-((1H-indazol-5-yl)methyl)-2,4-dimethyl-4,6-dihydro-5H-thiazolo[5',4':4,5]pyrrolo[2,3-d]pyridazin-5-one (18)



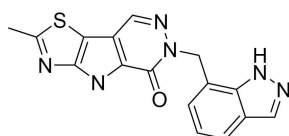
LCMS: m/z 351 (M+H)⁺. ¹H NMR (400 MHz, DMSO-d₆) δ 13.02 (s, 1H), 8.58 (s, 1H), 8.04 (s, 1H), 7.70 (s, 1H), 7.50 (d, 1H), 7.40 (d, 1H), 5.44 (s, 2H), 4.28 (s, 3H), 2.86 (s, 3H).

6-((1H-indazol-6-yl)methyl)-2,4-dimethyl-4H-thiazolo[5',4':4,5]pyrrolo[2,3-d]pyridazin-5(6H)-one (19)



LCMS: m/z 351 (M+H)⁺. ¹H NMR (400 MHz, DMSO-d₆) δ 12.96 (s, 1H), 8.59 (s, 1H), 8.03 (s, 1H), 7.71 (d, 1H), 7.42 (s, 1H), 7.13 (d, 1H), 5.48 (s, 2H), 4.27 (s, 3H), 2.86 (s, 3H).

6-((1H-indazol-7-yl)methyl)-2,4-dimethyl-4H-thiazolo[5',4':4,5]pyrrolo[2,3-d]pyridazin-5(6H)-one (20)



LCMS: m/z 351 (M+H)⁺. ¹H NMR (400 MHz, DMSO-d₆) δ 13.14 (s, 1H), 8.60 (s, 1H), 8.13 (s, 1H), 7.75–7.60 (m, 1H), 7.11–6.92 (m, 2H), 5.68 (s, 2H), 4.27 (s, 3H), 2.85 (s, 3H).

(eluent: PE/EtOAc=5/1) to give the desired product (4.7 g, 98.7% yield) as a yellow solid. LCMS: m/z 245 ($M+H$)⁺.

POCl₃ (22 mL, 0.24 mol) was added dropwise to a mixture of 2-chloro-4-methyl-4H-pyrrolo[2,3-d]thiazole-5-carboxylate (3 g, 12.3 mmol) in DMF (30 mL) in an ice-water bath. The reaction mixture was stirred at 100 °C overnight, then cooled, poured into ice water, and extracted with EtOAc. The combined organic layers were washed with brine, dried over anhydrous Na₂SO₄, and concentrated under reduced pressure. The residue was purified by column chromatography on silica gel (eluent: PE/EtOAc=5/1) to give the desired product (1.8 g, 53.9% yield) as a yellow solid. LCMS: m/z 273 ($M+H$)⁺.

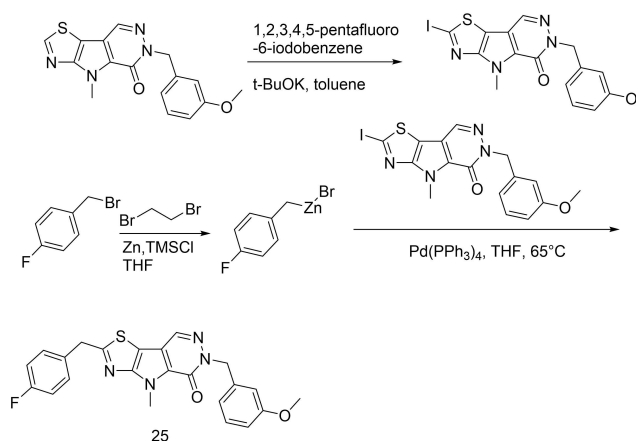
Hydrazine hydrate (23 mg, 0.73 mmol, 98% w/w) was added to a mixture of ethyl 2-chloro-6-formyl-4-methyl-4H-pyrrolo[2,3-d]thiazole-5-carboxylate (200 mg, 0.73 mmol) and AcOH (876 mg, 14.6 mmol) in ethanol (5 mL). The mixture was stirred at room temperature for 2 h, then poured into water and extracted with EtOAc. The combined organic layers were washed with brine, dried over anhydrous Na₂SO₄, and concentrated under reduced pressure. The residue was purified by column chromatography on silica gel (eluent: PE/EtOAc=2/1) to give the desired product (60 mg, 90% purity) as a yellow solid. LCMS: m/z 241 ($M+H$)⁺.

K₂CO₃ (103 mg, 0.75 mmol) was added to a mixture of 2-chloro-4-methyl-4H-thiazolo[5',4':4,5]pyrrolo[2,3-d]pyridazin-5(6H)-one (60 mg, 0.25 mmol) in DMF (5 mL). The mixture was stirred at that temperature for 10 min, followed by dropwise addition of 1-(chloromethyl)-3-methoxybenzene (46 mg, 0.3 mmol). The resulting mixture was stirred at 50 °C overnight, then poured into water and extracted with EtOAc. The combined organic layers were washed with brine, dried over anhydrous Na₂SO₄, and concentrated under reduced pressure. The residue was purified by prep-TLC to give the desired product (8 mg, 10% yield) as a yellow solid. LCMS: m/z 361 ($M+H$)⁺. ¹H NMR (400 MHz, DMSO-*d*₆) δ 8.65 (s, 1H), 7.24 (t, *J*=8.0 Hz, 1H), 6.86–6.83 (m, 3H), 5.32 (s, 2H), 4.25 (s, 3H), 3.72 (s, 3H).

Pd(PPh₃)₄ was added to a mixture of 2-chloro-6-(3-methoxybenzyl)-4-methyl-4H-thiazolo[5',4':4,5]pyrrolo[2,3-d]pyridazin-5(6H)-one (600 mg, 1.67 mmol) and tributyl(vinyl)stannane (1 mL, 3.4 mmol) in DMF (6 mL). The mixture was stirred at 100 °C overnight under N₂, then poured into water and extracted with EtOAc. The combined organic layers were washed with brine, dried over anhydrous Na₂SO₄, and concentrated under reduced pressure. The residue was purified by column chromatography on silica gel (eluent: PE/EtOAc=5/2) to give the desired product (410 mg, 68% yield) as a yellow solid. LCMS: m/z 353 ($M+H$)⁺. ¹H NMR (400 MHz, DMSO-*d*₆) δ 8.61 (s, 1H), 7.23 (t, *J*=8.0 Hz, 1H), 7.10 (dd, *J*=17.6, 10.8 Hz, 1H), 6.89–6.80 (m, 3H), 6.28 (d, *J*=17.6 Hz, 1H), 5.75 (d, *J*=11.2 Hz, 1H), 5.32 (s, 2H), 4.27 (s, 3H), 3.72 (s, 3H).

Pd/C (10 mg) was added to a mixture of 6-(3-methoxybenzyl)-4-methyl-2-vinyl-4H-thiazolo[5',4':4,5]pyrrolo[2,3-d]pyridazin-5(6H)-one (30 mg, 0.88 mmol) in MeOH (1 mL) and THF (1 mL) under N₂. The mixture was stirred under H₂ at room temperature for 1 h, then filtered through Celite. The filtrate was concentrated under reduced pressure and the residue was purified by prep-TLC to obtain the desired product (5 mg, 16.7% yield) as a white solid. LCMS: m/z 355 ($M+H$)⁺. ¹H NMR (400 MHz, DMSO-*d*₆) δ 8.56 (s, 1H), 7.23 (t, *J*=8.0 Hz, 1H), 6.89–6.78 (m, 3H), 5.32 (s, 2H), 4.26 (s, 3H), 3.72 (s, 3H), 3.17 (q, *J*=7.6 Hz, 2H), 1.38 (t, *J*=7.6 Hz, 3H).

2-(4-fluorobenzyl)-6-(3-methoxybenzyl)-4-methyl-4H-thiazolo[5',4':4,5]pyrrolo[2,3-d]pyridazin-5(6H)-one (25)



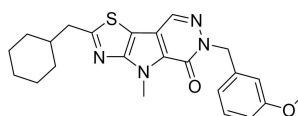
1,2,3,4,5-pentafluoro-6-iodobenzene (3.6 g, 12 mmol) was added to a stirred mixture of 6-(3-methoxybenzyl)-4-methyl-4,6-dihydro-5H-thiazolo[5',4':4,5]pyrrolo[2,3-d]pyridazin-5-one (1 g, 3 mmol) and *t*-BuOK (688 mg, 6 mmol) in toluene (30 mL) at room temperature. The reaction mixture was stirred at 135 °C for 4 h (oil bath was preheated) and then concentrated under reduced pressure. The residue was purified by column chromatography on silica gel (eluent: PE/EtOAc=6/1) to obtain the desired product (1 g, 72% yield). LCMS: m/z = 453 ($M+H$)⁺. ¹H NMR (400 MHz, DMSO-*d*₆) δ 8.61 (s, 1H), 7.23 (t, 1H), 6.88–6.80 (m, 3H), 5.31 (s, 2H), 4.26 (s, 3H), 3.71 (s, 3H).

Zn powder (1300 mg, 20 mmol) was added to a 25 mL, three-necked, round-bottom flask. The mixture was degassed under high vacuum and back-purged with N₂ three times. Dry THF (15 mL), trimethylsilyl chloride (108 mg, 1 mmol), and 1,2-dibromoethane (186 mg, 1 mmol) were added via syringe at room temperature. The suspension was heated to 65 °C for 30 min, then cooled to 0 °C, followed by dropwise addition of 1-(bromomethyl)-4-fluorobenzene (1.89 g, 10 mmol). The resulting mixture was stirred at room temperature for 1.5 h. The supernatant solution was directly used for the next step.

2-iodo-6-(3-methoxybenzyl)-4-methyl-4H-thiazolo[5',4':4,5]pyrrolo[2,3-d]pyridazin-5(6H)-one (100 mg, 0.22 mmol) and Pd(PPh₃)₄ (25.4 mg, 10 mol%) were added to a 25 mL, three-necked, round-bottom flask. The flask was degassed under high vacuum and back-purged with N₂ three times. The supernatant solution of (4-fluorobenzyl)zinc(II) bromide (6 mL) was added via syringe to the flask. The resulting mixture was stirred under N₂ at 65 °C for 0.5 h, then concentrated under reduced pressure. The residue was purified by prep-TLC to give the desired product (6 mg, 6% yield). LCMS: m/z = 435 ($M+H$)⁺. ¹H NMR (400 MHz, DMSO-*d*₆) δ 8.53 (s, 1H), 7.75–7.50 (m, 1H), 7.47 (s, 2H), 7.23 (s, 3H), 6.84 (s, 2H), 5.31 (s, 2H), 4.52 (s, 2H), 4.26 (s, 3H), 3.71 (s, 3H).

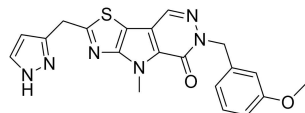
The procedure above was used to produce compounds **24** and **26** using the appropriate starting materials.

2-(cyclohexylmethyl)-6-(3-methoxybenzyl)-4-methyl-4H-thiazolo[5',4':4,5]pyrrolo[2,3-d]pyridazin-5(6H)-one (24) was synthesized similarly using Negishi coupling with (bromomethyl)cyclohexane.



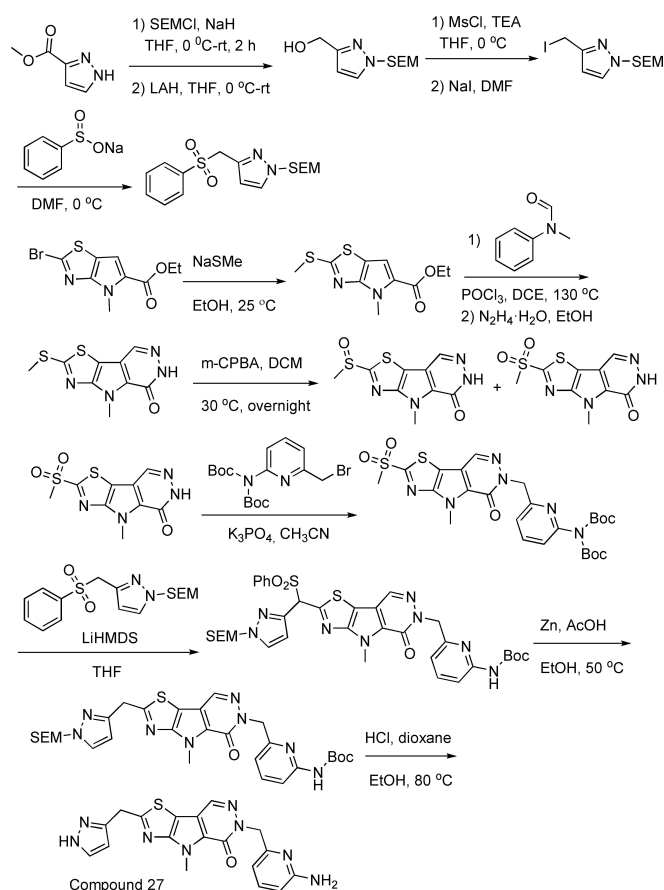
LCMS: m/z 423 ($M+H$)⁺. ¹H NMR (400 MHz, DMSO-*d*₆) δ 8.55 (s, 1H), 7.23 (t, $J=8.0$ Hz, 1H), 6.84–6.82 (m, 3H), 5.32 (s, 2H), 4.26 (s, 3H), 3.71 (s, 3H), 3.02 (d, $J=6.8$ Hz, 2H), 1.76–1.59 (m, 5H), 1.25–1.00 (m, 6H).

2-((1H-pyrazol-3-yl)methyl)-6-(3-methoxybenzyl)-4-methyl-4,6-dihydro-5H-thiazolo[5',4':4,5]pyrrolo[2,3-d]pyridazin-5-one (26) was synthesized similarly using Negishi coupling with tert-butyl 3-(bromomethyl)-1H-pyrazole-1-carboxylate.



LCMS: m/z 407 ($M+H$)⁺. ¹H NMR (400 MHz, DMSO-*d*₆) δ 12.79 (s, 1H), 8.54 (s, 1H), 8.43 (s, 1H), 7.73 (s, 1H), 7.23 (dd, 1H), 6.84–6.74 (m, 2H), 6.26 (d, 1H), 5.31 (s, 2H), 4.49 (s, 2H), 4.27 (s, 3H), 3.71 (s, 3H).

2-((1H-pyrazol-3-yl)methyl)-6-((6-aminopyridin-2-yl)methyl)-4-methyl-4H-thiazolo[5',4':4,5]pyrrolo[2,3-d]pyridazin-5(6H)-one (27)



NaSMc (240 mg, 3.5 mmol) was added to a mixture of ethyl 2-bromo-4-methyl-4H-pyrrolo[2,3-d]thiazole-5-carboxylate (500 mg, 1.73 mmol) in EtOH (10.0 mL). The reaction mixture was stirred at 25 °C for 3 h, then quenched with ice water and extracted with DCM. The combined organic layers were washed with brine, dried over anhydrous Na₂SO₄, and concentrated under reduced pressure to obtain the desired product (460 mg), which was directly used in the next step without any purification. LCMS: m/z 257 ($M+H$)⁺.

POCl₃ (550 mg, 3.6 mmol) was added to a solution of ethyl 4-methyl-2-(methylthio)-4H-pyrrolo[2,3-d]thiazole-5-carboxylate

(460 mg, 1.8 mmol) and N-methyl-N-phenylformamide (490 mg, 3.6 mmol) in 1,2-dichloroethane (DCE) (10 mL). The resulting mixture was stirred at 130 °C for 3 h, then quenched with ice water and extracted with DCM. The combined organic layers were washed with brine, dried over anhydrous Na₂SO₄, and concentrated under reduced pressure. The residue was purified by column chromatography on silica gel (eluent: PE/EtOAc=8/1) to give the desired product (320 mg, 63% yield). LCMS: m/z 285 ($M+H$)⁺.

N₂H₄·H₂O (2 mL, 98% weight [wt]) was added to a solution of ethyl 6-formyl-4-methyl-2-(methylthio)-4H-pyrrolo[2,3-d]thiazole-5-carboxylate (300 mg, 1.06 mmol) in EtOH (5.0 mL). The reaction mixture was stirred at room temperature for 1 h, then heated to 60 °C overnight and subsequently cooled down. The solid was collected by filtration and dried under high vacuum to obtain the desired product (180 mg, 67% yield). LCMS: m/z 253 ($M+H$)⁺. ¹H NMR (400 MHz, DMSO-*d*₆) δ 12.61 (s, 1H), 8.48 (s, 1H), 4.22 (s, 3H), 2.81 (s, 3H).

Meta-chloroperoxybenzoic acid (m-CPBA) (61.5 g, 3 eq) was added to a three-necked flask containing 4-methyl-2-(methylthio)-4,6-dihydro-5H-thiazolo[5',4':4,5]pyrrolo[2,3-d]pyridazin-5-one (30 g, 0.119 mol, 1.0 eq) in DCM (600 mL) at 20 °C in three portions. The mixture was stirred at 30 °C overnight; LCMS indicated 100% consumption of starting material, forming 20% sulfoxide and 80% sulfone. The mixture was cooled to room temperature and another portion of m-CPBA (1.0 eq) was added. The reaction mixture was stirred at 30 °C for 2 h; LCMS indicated sulfoxide (LCMS: m/z 269 ($M+H$)⁺) < 8%. The mixture was cooled to room temperature and filtered. The filtered cake was suspended in MeOH (500 mL) and stirred at room temperature for 1 h. Solid was collected by filtration, washed with EtOAc, and dried in a vacuum to afford 28 g of a mixture of 5% sulfoxide and 95% sulfone. The mixture was suspended in DMSO (600 mL), heated to approximately 120–130 °C to form a clear solution, and cooled to room temperature, leading to formation of a solid precipitate. The mixture was filtered and dried to provide 23 g of pure 4-methyl-2-(methylsulfonyl)-4,6-dihydro-5H-thiazolo[5',4':4,5]pyrrolo[2,3-d]pyridazin-5-one, LCMS: m/z 285 ($M+H$)⁺. ¹H NMR (400 MHz, DMSO) δ 12.87 (s, 1H), 8.69 (s, 1H), 4.32 (s, 3H), 3.56 (s, 3H).

At 0 °C under N₂ atmosphere, NaH (20.7 g, 0.864 mol, 60%) was added to a stirred solution of methyl 1H-pyrazole-3-carboxylate (90 g, 0.72 mol) in THF (1 L). The resulting mixture was slowly warmed to room temperature and stirred for 1 h. The reaction mixture was then cooled back to 0 °C and SEMCl (152 mL, 0.842 mol) was added dropwise. Stirring continued for another 2 h, when the mixture was quenched with saturated NH₄Cl and extracted with EtOAc (3×). The combined organic layers were washed with brine and dried over Na₂SO₄. Solvents were removed under vacuum to provide 210 g of crude product, which was used in the next step without purification.

At 0 °C under an N₂ atmosphere, the crude methyl 1-((2-(trimethylsilyloxy)methyl)-1H-pyrazol-3-yl)methyl-1H-pyrazole-3-carboxylate (76 g) was added to the suspension of LAH (16.9 g, 0.44 mol) in THF (760 mL). The resulting mixture was slowly warmed to room temperature and stirred for 1 h. The reaction mixture was cooled back to 0 °C, and H₂O (15.6 mL), 10% NaOH (15.6 mL), and H₂O (15.6 mL) were added in succession. The resulting mixture was filtered through a pad of Celite and washed with methyl tert-butyl ether (MTBE) (4×). The combined organic fractions were dried over Na₂SO₄. Solvents were removed under reduced pressure to provide crude product (69.4 g), which was used in the next step without purification. LCMS: m/z 229 ($M+H$)⁺.

At 0 °C under an N₂ atmosphere, triethylamine (TEA) (55.4 mL, 0.393 mol) followed by MsCl (24.0 mL, 0.314 mol) was added to a stirred solution of (1-((2-(trimethylsilyl)ethoxy)methyl)-1H-pyrazol-3-yl)methanol (61.5 g, theoretically 0.262 mol) in THF (310 mL). The reaction was warmed to room temperature and stirred for 1 h before the introduction of NaI (196.5 g, 1.31 mol, in 310 mL DMF). The resulting mixture was stirred for 1 h, quenched with ice water, and extracted with MTBE (3×). The combined organic layers were washed with saturated Na₂S₂O₃ and then with brine, dried over Na₂SO₄, and concentrated to provide 77.5 g crude product used in the next step without purification. LCMS: m/z 339 (M + H)⁺.

At 0 °C under an N₂ atmosphere, sodium benzenesulfinate (53.5 g, 0.32 mol) was added to a stirred solution of 3-(iodomethyl)-1-((2-(trimethylsilyl)ethoxy)methyl)-1H-pyrazole (77.5 g, theoretically 0.229 mol) in DMF (600 mL) and then was stirred for 1 h at 0 °C. After warming to room temperature, the reaction mixture was quenched with ice water and saturated Na₂S₂O₃, and then extracted with EtOAc (3×). The combined organic layers were washed with saturated NaHCO₃ and then with brine successively and dried over Na₂SO₄. Solvents were removed under vacuum, and the residue was purified by flash chromatography (silica gel, 20%~70% EtOAc in petroleum ether) to provide 56.7 g product 3-((phenylsulfonyl)methyl)-1-((2-(trimethylsilyl)ethoxy)methyl)-1H-pyrazole as a light-yellow oil. LCMS: [M + H]⁺ 353. ¹H NMR (400 MHz, DMSO) δ 7.85–7.77 (m, 4H), 7.62 (dd, 2H), 6.19 (d, 1H), 5.35 (d, 2H), 4.70 (d, 2H), 3.44–3.38 (m, 2H), 0.88–0.77 (m, 2H), –0.01 (s, 9H).

A mixture of 4-methyl-2-(methylsulfonyl)-4H-thiazolo[5',4':4,5]-pyrrolo[2,3-d]pyridazin-5(6H)-one (7.5 g, 26.4 mmol) and K₃PO₄ (8.3 g, 39.3 mmol) in anhydrous MeCN (300 mL) was stirred at 70 °C for 1 h under N₂. A solution of tert-butyl (6-(bromomethyl)pyridin-2-yl)(tert-butoxycarbonyl)carbamate (11.2 g, 29.0 mmol) in MeCN (30 mL) was then added. After stirring at 70 °C for 2.5 h under N₂, the reaction mixture was quenched with saturated NH₄Cl and extracted with EtOAc (300 mL×3). The combined organic layers were washed with water and then brine, dried over Na₂SO₄, filtered, and the organic phase was concentrated. The crude product was purified by flash chromatography (silica gel, 0–50% ethyl acetate in petroleum ether) to give tert-butyl (tert-butoxycarbonyl)(6-((4-methyl-2-(methylsulfonyl)-5-oxo-4,5-dihydro-6H-thiazolo[5',4':4,5]pyrrolo[2,3-d]pyridazin-6-yl)methyl)-pyridin-2-yl)carbamate (5.5 g, 32% yield). LCMS (ESI) found: 591.1 (M + H)⁺.

LiHMDS (50.0 mL, 1 M in THF) at –40 °C under argon was added to a stirred mixture of 3-((phenylsulfonyl)methyl)-1-((2-(trimethylsilyl)ethoxy)methyl)-1H-pyrazole (11.9 g, 33.8 mmol) in anhydrous THF (200 mL). After 10 min, the mixture was warmed to 10 °C and stirred for 1 h, then tert-butyl (tert-butoxycarbonyl)(6-((4-methyl-2-(methylsulfonyl)-5-oxo-4,5-dihydro-6H-thiazolo[5',4':4,5]pyrrolo[2,3-d]pyridazin-6-yl)methyl)pyridin-2-yl)carbamate (9.1 g, 15.4 mmol in 35 mL THF) was added. The reaction was stirred at 10 °C for another 30 min. The reaction mixture was poured into aqueous NH₄Cl and extracted with EtOAc (200 mL ×3). The combined organic layers were washed with water and brine, dried over anhydrous Na₂SO₄, and concentrated. The crude product was purified by flash chromatography (silica gel, 0–50% ethyl acetate in petroleum ether) to give tert-butyl (6-((4-methyl-5-oxo-2-((phenylsulfonyl)(1-((2-(trimethylsilyl)ethoxy)methyl)-1H-pyrazol-3-yl)methyl)-4H-thiazolo[5',4':4,5]pyrrolo[2,3-d]pyridazin-6(5H)-yl)methyl)pyridin-2-yl)carbamate (6.6 g, 56% yield). LCMS (ESI) found: 763.2 (M + H)⁺.

A solution of tert-butyl (6-((4-methyl-5-oxo-2-((phenylsulfonyl)(1-((2-(trimethylsilyl)ethoxy)methyl)-1H-pyrazol-3-yl)methyl)-4H-thiazolo[5',4':4,5]pyrrolo[2,3-d]pyridazin-6(5H)-yl)methyl)pyridin-2-yl)carbamate (6.0 g, 7.86 mmol) in EtOH/AcOH (35 mL/50 mL) was

heated to 50 °C and vigorously stirred in the presence of Zn (2.55 g, 117.9 mmol) for 40 min. Additional Zn was added every 40 min (2.55 g, twice, with monitoring by TLC/LCMS to avoid by-product and over-reduced product). The solution was filtered and the filter cake was washed with DCM. The filtrate was partly evaporated, neutralized with saturated NaHCO₃ solution, dried over MgSO₄, and the solvent was removed under vacuum. The crude product was purified by flash chromatography (silica gel, DCM:MeOH=40:1) to give tert-butyl (6-((4-methyl-5-oxo-2-((1-((2-(trimethylsilyl)ethoxy)methyl)-1H-pyrazol-3-yl)methyl)-4,5-dihydro-6H-thiazolo[5',4':4,5]pyrrolo[2,3-d]pyridazin-6-yl)methyl)-pyridin-2-yl)carbamate (3.1 g, 63% yield). LCMS (ESI) found: 623.3 (M + H)⁺.

HCl (30 mL, 4 M in dioxane) was added to a mixture of tert-butyl (6-((4-methyl-5-oxo-2-((1-((2-(trimethylsilyl)ethoxy)methyl)-1H-pyrazol-3-yl)methyl)-4,5-dihydro-6H-thiazolo[5',4':4,5]pyrrolo[2,3-d]pyridazin-6-yl)methyl)pyridin-2-yl)carbamate (3.0 g, 4.8 mmol) in ethanol (30 mL). The reaction mixture was stirred at 80 °C for 40 min. The reaction mixture was cooled to room temperature, filtered, and the solid was collected, suspended in water, and neutralized with aqueous NaHCO₃ at 10 °C. The reaction mixture was filtered to give the desired compound 2-((1H-pyrazol-3-yl)methyl)-6-((6-aminopyridin-2-yl)methyl)-4-methyl-4H-thiazolo[5',4':4,5]pyrrolo[2,3-d]pyridazin-5(6H)-one (1.5 g, 78% yield). LC-MS (ESI) found: 393.2 (M + H)⁺. ¹H NMR (400 MHz, DMSO-*d*₆) δ 12.78 (s, 1H), 8.53 (s, 1H), 7.72 (s, 1H), 7.25 (dd, 1H), 6.33–6.24 (m, 2H), 6.08 (d, 1H), 5.90 (s, 2H), 5.19 (s, 2H), 4.49 (s, 2H), 4.26 (s, 3H).

Other Contributions

We thank the following non-authors for their valuable contributions to the study:

- Sebastien Ronseaux, s.ronseaux@mac.com (contributions–design of the drug metabolism and pharmacokinetics [DMPK] experiments, collection of DMPK data, and write-up of DMPK results)
- Giovanni Cianchetta, gcianchetta@recludix.com (contribution–computational chemistry support, helped use the structures to design new compounds including AG-946 together with Tao Liu, co-inventor on patents describing the compounds)
- Penelope A. Kosinski, pakosins@yahoo.com (contribution–developed the cellular assays, analyzed data, and helped with early draft)
- Zhijia Sui, zsui@proteovant.com (contribution–intellectual contribution to the project strategy and compound designs, co-inventor on patents describing the compounds)
- Stefan Gross, Stefan.GROSS@servier.com (contribution–intellectual contribution to the assay design and compound selection)
- Zhijia of Biortus, zhijia.lv@wuxibiortus.com (contribution–CRO scientist for X-ray crystallography support)
- Huachun Tang at CP, hchtang@chempartner.com (contribution–CRO scientist for biochemical assay support)
- Fei Teng at CP, fteng1@chempartner.com (CRO scientist for biochemical assay support)

- ix. Scott A. Biller, scottabiller@gmail.com (contribution—intellectual contribution to the drugging strategy, compound selection, and progression).
- x. Kris Depew, Kris.Depew@agios.com (contribution—write-up of chemistry sections, revision, and editing of the manuscript).

Supporting Information

The Supporting Information is available free of charge online. Supplemental data include one table and three figures.

Author Contributions

T.L., A.K.P., and E.T.J. participated in the conceptualization of research goals; development or design of methodology; provision of resources; supervision and administration of the research; conduct of the investigation; data curation; validation and formal analysis of data; and visualization, writing, and reviewing of the manuscript. L.J. participated in the development or design of methodology; supervision and administration of the research; conduct of the investigation; data curation; validation and formal analysis of data; and visualization, writing, and reviewing of the manuscript. D.H. participated in the visualization, writing, and reviewing of the manuscript. C.K. participated in the conceptualization of research goals; supervision of the research; and writing and reviewing of the manuscript. L.D. participated in the conceptualization of research goals; supervision and administration of the research; and writing and reviewing of the manuscript.

Acknowledgements

This study was funded by Agios Pharmaceuticals, Inc.

Conflict of Interests

T.L. was an employee of Agios Pharmaceuticals, Inc. at time of research; is named as a co-inventor on related patents, including those associated with AG-946; and reports holding stock in Agios Pharmaceuticals, Inc. A.K.P. was an employee of Agios Pharmaceuticals, Inc. at time of research; is presently an employee of Atavistik Bio, a privately held biotechnology company; is named as a co-inventor on related patents, including those associated with AG-946; and reports holding stock in Agios Pharmaceuticals, Inc. E.T.J. was an employee of Agios Pharmaceuticals, Inc. at time of research; is presently an employee of Novartis; and reports holding stock in both Agios Pharmaceuticals, Inc. and Novartis. L.J. was a consultant for Agios Pharmaceuticals, Inc. at time of research and reports no other conflicts of interest. D.H. is a full-time employee and stockholder of Agios Pharmaceuticals, Inc. C.K. was an employee of Agios Pharmaceuticals, Inc. at time of research; is named as a

co-inventor on related patents, including those associated with AG-946; and reports holding stock in Agios Pharmaceuticals, Inc. L.D. is an independent consultant for Agios Pharmaceuticals, Inc.; is named as a co-inventor on related patents, including those associated with AG-946; and reports no other conflicts of interest.

Data Availability Statement

Qualified researchers may request access to related clinical study documents. Please send your data sharing requests to datasharing@agios.com. The following considerations will be taken into account as part of the review:

1. Ability for external researcher to re-identify trial participants such as small rare disease trials or single-center trials.
2. Language used in data and requested documents (e.g., English or other).
3. Informed consent language with respect to allowance for data sharing.
4. Plan to re-evaluate safety or efficacy data summarized in the approved product labeling.
5. Potential conflict of interest or competitive risk

Keywords: AG-946 · allosterism · medicinal chemistry · pharmacokinetics · pyruvate kinase activator

- [1] R. van Wijk, W. van Solinge, *Blood* **2005**, *106*, 4034–4042.
- [2] F. A. Oski, H. Bowman, *Br. J. Haematol.* **1969**, *17*, 289–297.
- [3] M. A. E. Rab, J. Bos, B. A. van Oirschot, S. van Straaten, P. A. Kosinski, V. Chubukov, H. Kim, H. Mangus, R. E. G. Schutgens, G. Pasterkamp, L. Dang, C. Kung, E. J. van Beers, R. van Wijk, *Blood* **2021**, *137*, 2997–3001.
- [4] U. Platzbecker, L. C. Hofbauer, G. Ehninger, K. Hölig, *Leuk. Res.* **2012**, *36*, 525–536.
- [5] a) P. Boivin, C. Galand, M. Audollent, *Pathol. Biol. (Paris)* **1970**, *18*, 175–187; b) A. Kahn, J. Marie, J. F. Bernard, D. Cottreau, P. Boivin, *Clin. Chim. Acta.* **1976**, *71*, 379–387.
- [6] a) B. Fattizzo, C. Vercellati, A. Marcello, M. Bortolotti, A. Zaninoni, E. Fermo, P. Bianchi, W. Barcellini, *Blood* **2022**, *140*, 4016–4017; b) B. Fattizzo, C. Vercellati, A. Marcello, P. Patel, M. Wind-Rotolo, L. Pettine, S. Leoni, E. Fermo, P. Bianchi, A. Zaninoni, W. Barcellini, in *European Hematology Association Frankfurt, Germany*, **2023**.
- [7] a) K. H. M. Kuo, D. M. Layton, A. Lal, H. Al-Samkari, P. A. Kosinski, B. Tong, J. H. Estep, K. Uhlig, E. P. Vichinsky, *Blood* **2022**, *140*, 2479–2480; b) K. H. M. Kuo, D. M. Layton, A. Lal, H. Al-Samkari, J. Bhatia, P. A. Kosinski, B. Tong, M. Lynch, K. Uhlig, E. P. Vichinsky, *Lancet* **2022**, *400*, 493–501.
- [8] W. A. Eaton, H. F. Bunn, *Blood* **2017**, *129*, 2719–2726.
- [9] Z. B. Rose, *Biochem. Biophys. Res. Commun.* **1976**, *73*, 1011–1017.
- [10] a) X. Dai Gurov, E. Merica, V. Iyer, A. Claeys, S. Patil, R. Urbstonaitis, J. Xiao, M. U. Callaghan, *Blood* **2022**, *140*, 5426–5427; b) J. de Wilde, T. Ruiter, B. A. van Oirschot, J. Jans, L. Dang, M. Wind-Rotolo, W. W. van Solinge, A. van Rhenen, R. van Wijk, M. Rab, in *European Hematology Association, Frankfurt, Germany*, **2023**; c) H. Yang, E. Merica, Y. Chen, M. Cohen, R. Goldwater, P. A. Kosinski, C. Kung, Z. J. Yuan, L. Silverman, M. Goldwasser, B. A. Silver, S. Agresta, A. J. Barbier, *Clin. Pharmacol. Drug Dev.* **2019**, *8*, 246–259.
- [11] a) R. van Zwieten, B. A. van Oirschot, M. Veldhuis, J. G. Dobbe, G. J. Streekstra, W. W. van Solinge, R. E. Schutgens, R. van Wijk, *Am. J. Hematol.* **2015**, *90*, e35–e39; b) N. Alli, M. Coetzee, V. Louw, B. van Rensburg, G. Rossouw, L. Thompson, S. Pissard, S. L. Thein, *Hematology* **2008**, *13*, 369–372.
- [12] J. K. Jiang, M. B. Boxer, M. G. Vander Heiden, M. Shen, A. P. Skoumbourdis, N. Southall, H. Veith, W. Leister, C. P. Austin, H. W. Park, J. Inglesse,

- L. C. Cantley, D. S. Auld, C. J. Thomas, *Bioorg. Med. Chem. Lett.* **2010**, *20*, 3387–3393.
- [13] D. Gramec, L. Peterlin Masic, M. Sollner Dolenc, *Chem. Res. Toxicol.* **2014**, *27*, 1344–1358.
- [14] P. R. Lazzara, T. W. Moore, *RSC Med. Chem.* **2020**, *11*, 18–29.
- [15] G. Scapin, S. B. Patel, C. Chung, J. P. Varnerin, S. D. Edmondson, A. Mastracchio, E. R. Parmee, S. B. Singh, J. W. Becker, L. H. van der Ploeg, M. R. Tota, *Biochemistry* **2004**, *43*, 6091–6100.
- [16] A. F. Stepan, D. P. Walker, J. Bauman, D. A. Price, T. A. Baillie, A. S. Kalgutkar, M. D. Aleo, *Chem. Res. Toxicol.* **2011**, *24*, 1345–1410.
- [17] a) L. M. Lima, E. J. Barreiro, *Curr. Med. Chem.* **2005**, *12*, 23–49; b) N. A. Meanwell, *J. Med. Chem.* **2011**, *54*, 2529–2591.
- [18] a) P. Bhutani, G. Joshi, N. Raja, N. Bachhav, P. K. Rajanna, H. Bhutani, A. T. Paul, R. Kumar, *J. Med. Chem.* **2021**, *64*, 2339–2381; b) M. Marinescu, *Int. J. Pharm. Bio. Sci.* **2017**, *8*, 338–355.
- [19] C. Kung, J. Hixon, P. A. Kosinski, G. Cianchetta, G. Histen, Y. Chen, C. Hill, S. Gross, Y. Si, K. Johnson, B. DeLaBarre, Z. Luo, Z. Gu, G. Yao, H. Tang, C. Fang, Y. Xu, X. Lv, S. Biller, S. M. Su, H. Yang, J. Popovici-Muller, F. Salituro, L. Silverman, L. Dang, *Blood* **2017**, *130*, 1347–1356.
- [20] Z. Otwinowski, W. Minor, *Methods Enzymol.* **1997**, *276*, 307–326.
- [21] A. J. McCoy, R. W. Grosse-Kunstleve, P. D. Adams, M. D. Winn, L. C. Storoni, R. J. Read, *J. Appl. Crystallogr.* **2007**, *40*, 658–674.
- [22] A. W. Schuttelkopf, D. M. van Aalten, *Acta Crystallogr. Sect. D* **2004**, *60*, 1355–1363.
- [23] P. Emsley, B. Lohkamp, W. G. Scott, K. Cowtan, *Acta Crystallogr. Sect. D* **2010**, *66*, 486–501.
- [24] P. D. Adams, P. V. Afonine, G. Bunkoczi, V. B. Chen, I. W. Davis, N. Echols, J. J. Headd, L. W. Hung, G. J. Kapral, R. W. Grosse-Kunstleve, A. J. McCoy, N. W. Moriarty, R. Oeffner, R. J. Read, D. C. Richardson, J. S. Richardson, T. C. Terwilliger, P. H. Zwart, *Acta Crystallogr. Sect. D* **2010**, *66*, 213–221.

Manuscript received: October 17, 2023

Revised manuscript received: December 14, 2023

Accepted manuscript online: December 18, 2023

Version of record online: February 2, 2024